1-1-2009

Identification Of A Novel Gene Altered In The RQ1 Mutant Strain Affecting Motor Axon Migration In Caenorhabditis Elegans

Haider Z. Naqvi
Ryerson University

IDENTIFICATION OF A NOVEL GENE ALTERED IN THE *RQ1* MUTANT STRAIN AFFECTING MOTOR AXON MIGRATION IN *CAENORHABDITIS ELEGANS*

by

Zafaryab Haider Naqvi, B.Sc,

Ryerson University

Toronto, 2009

A thesis presented to Ryerson University

in partial fulfillment of the requirements for the degree of

Master of Science in the Program of

Molecular Science

Toronto, Ontario, Canada, 2009

Author's Declaration

I hereby declare that I am the sole author of this thesis.

I authorize Ryerson University to lend this thesis to other institutions or individuals for the purpose of scholarly research.

Zafaryab Haider Naqvi

I further authorize Ryerson University to reproduce this thesis by photocopying or by other means, in total or in part, at the request of other institutions or individuals for the purpose of scholarly research.

Zafaryab Haider Naqvi

Abstract

Zafaryab Naqvi

Identification of a novel gene altered in the *rq1* mutant strain affecting motor axon migration in *Caenorhabditis elegans*

Master of Science

Molecular Science

Ryerson University, Toronto, 2009

Novel genetic enhancer screens were conducted targeting mutants involved in the guidance of axons of the DA and DB classes of motor neurons in *C. elegans*. These mutations are expected in genes that function in parallel to the *unc-6*/Netrin pathway. The screen was conducted in an *unc-5(e53)* genetic background and enhancers of the axon guidance defects caused by the absence of UNC-5 were identified. Three mutants were previously identified in this screen called *rq1, rq2* and *rq3* and two additional mutants called *H2-4* and *M1*-3, were isolated in this study. In order to identify the gene affected by the *rq1* mutation, wild-type copies of genes in the mapped *rq1* mutation region were injected into the mutants to rescue the phenotypic defects. There is a strong indication that the gene of interest is a novel gene called H04D03.1. Promising results indicate that the H04D03.1 protein also works in germ-line apoptosis.

Acknowledgements

I would first like to thank Dr. Marie Killeen for giving me the opportunity to work with her on this project, for guiding me through the numerous hurdles that I encountered, and for enhancing my knowledge of genetics and biochemistry. I would also like to thank Stephanie Sybingco, Matt Bueno, Sang Park, and Ganna Kholkina for teaching me all the protocols that are used in the lab and for providing the background information that I needed to finish my study. Viktoria Serdetchnaia has been instrumental in this study and her work was crucial for finding the *rq1* gene. Tracy Lakraj, Rozia Rezania, and Andriana Guigova have provided tremendous support in characterizing the *rq1* mutant and their work cannot be understated.

I would also like to thank the Roy Lab and the Culotti Lab for providing the necessary reagents and equipment that were used in this study. Also deserving thanks are Wendy Johnston, Kristie Jolliffe, Leslie MacNeil and Takahiro Kawano for great advice on several problems that I encountered during this study.

A big thank you for my family and friends especially my wife Farheen for providing essential support and for informally co-supervising me in my work. And to little Hasnain Ali, thank you for not destroying my laptop.

Table of contents: **Page**

Page

List of Tables

Page

List of Figures

Page

Page

List of Abbreviations

AO	Acridine Orange
AP	Anterior-Posterior guidance
Apaf	Apoptosis Protease Activating Factor
AVM	Anterior Ventral Mechanosensory neuron
CED	Cell Engulfment Defective
CDD	NCBI Conserved Domain Database
DA/DB	Dorsal A/Dorsal B class of motor neurons
DCC	Deleted in Colorectal Cancer
DD	Death Domain
DIC	Differential Interference Contrast
DNA	DeoxyriboNucleic Acid
dsRNA	Double-Stranded RiboNucleic Acid
DV	Dorsal-Ventral
DTC	Distal Tip Cell
EGL	EGg Laying defective
EMS	EthylMethaneSulfonate
GFP	Green Fluorescent Protein
LG	Linkage Group
LTR	Long Terminal Repeat
MEC	MEChanosensory neuron
MYO	MYOsin protein
N2	Bristol strain
NGM	Nematode Growth Media
PCR	Polymerase Chain Reaction
PKC	Protein Kinase C
PKT2	Protein Tyrosine Kinase 2
rq	Killeen's Lab mutant designation
RE	Restriction Endonuclease
RNAi	RiboNucleic Acid Interference
SAX	Sensory AXon guidance
SLT	Slit
SNP	Single Nucleotide Polymorphism
SFK	Src-Family Kinase
Tg	Transgenic
TGF-β	Transforming Growth Factor β
UNC	UNCoordinated
UV	UltraViolet light
Y2H	Yeast-two-Hybrid screen
YFP	Yellow Fluorescence Protein
ZEN	Zygotic ENclosure defective

1. Introduction

In order to fully understand the mechanics of nervous system development, scientists have made use of several model organisms with fully functional nervous systems. An organism which has a nervous system that uses proteins homologous to that of the human brain is fundamental in divulging the intricacies of how neurons form networks that transmit and receive signals and respond to environmental stresses. Among these model organisms is a simple nematode called *Caenorhabditis elegans (C. elegans)*. Work on this microscopic, non-parasitic nematode has revealed some of the major proteins involved in nervous system development. This current work was conducted to identify a novel protein that could be implicated in nervous system development.

1.1 Nervous system of *C. elegans*

Compared to other model organisms, *C. elegans* has a relatively simple nervous system containing only 302 neurons in the hermaphrodite (Brenner, 1974). Similar to what is seen in higher organisms, *C. elegans* has three types of neurons; sensory, motor, and interneurons (White, 1976). Most sensory neurons are concentrated in the head where they are divided into mechanosensory and chemosensory neurons also known as amphids. A large number of axons exit the pharyngeal ganglia and go along the ventral part of the worm forming a ventral nerve cord. Motor neurons have their cell bodies lined on the ventral nerve cord and send axons in the dorsal direction around the body of the worm between the basement and hypodermal membranes. Upon reaching the dorsal side of the worm, these motor axons form a dorsal nerve cord by either going in an anterior or

posterior direction along the body wall, depending on the class of motor neuron (White, 1976).

There are 5 classes of motor neurons which are A, B, C, AS, and D. This work will focus on classes A and B, more specifically subclasses Dorsal A (DA) and Dorsal B (DB) (White, 1976). DA neurons cause backward movements while DB neurons cause forward movement (White, 1976). Neurons belonging to both these classes are morphologically the same except for one anatomical difference. Subclass DA neurons, project axons in the anterior direction and their processes also go to the anterior upon reaching the dorsal cord before they synapse (Fig. 1.1.1). In subclass DB, axons are also projected in the anterior direction but upon reaching the dorsal nerve cord, these processes migrate towards the posterior end where they synapse (Figure 1.1.1) (White, 1976).

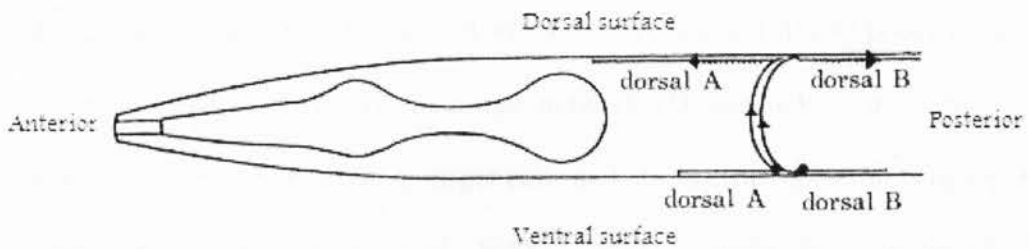

Figure 1.1.1: Above image shows DA and DB motor axon migration in the body of nematode *C. elegans*. Cell bodies for both types of neurons are at the ventral nerve cord on the ventral surface of the worm where they send axons out towards the dorsal surface to synapse with muscles involved in forward and backward movement (White, 1976)

Another difference between the two subclasses concerns the source of their incoming signals. DA neurons receive signals through the gap junctions of α-inter-neurons and δ-inter-neurons, whereas DB neurons get their stimuli through β- and γ-inter-neurons. After receiving these signals, motor neurons transmit them through neuromuscular junctions which are located at the basement membrane of the animal (White, 1976). The neuro muscular synapses of the DA and DB are with the dorsal muscles through inter-neurons (White, 1976). If these DA/DB motor neurons fail to make it to their specific neuromuscular junctions, the animal understandably has difficulty with locomotion and becomes uncoordinated (Unc).

1.2 Molecular guidance cues for DA/DB motor axons:

Active axonal growth-cones are found at the tips of growing axons. They are guided by extracellular molecules present in the matrix between the hypodermis and the basal membrane that contains the neuronal network (Hedgecock *et al*, 1990). These guidance cues are released by remote target cells and act as either attractants or repellents of the growth-cone (Dodd and Jessel, 1988). Guidance molecules can be identified genetically by treating the animals with mutagens and picking those mutants which display incorrect axonal trajectories of target neurons. Target neurons can be observed by the expression of appropriate proteins such as neuronal UNC-129/TGFβ which is only expressed in DA and DB motor neurons. Once the mutant gene is identified, it theoretically should be implicated in playing a role in axon guidance and neural network formation (Hedgecock *et al*, 1990). Using this technique, three genes were identified that

affect guidance of the DA and DB motor axons. These genes were *unc-5*, *unc-6*, and *unc-40* where 'Unc' indicates that these mutations cause the animal to become uncoordinated. Earlier, it was established through double mutant analysis that *unc-6* depends on *unc-5* and *unc-40* for its function and *unc-5* and most *unc-40* functions depend on the presence and function of the UNC-6 protein (Hedgecock *et al*, 1990). In regards to axon migration, these genes regulate migration mainly along the dorso-ventral axis of the animal. The DA and DB motor neurons fall into this category and hence their migration patterns are affected if any of the three genes are defective. UNC-6 is a laminin-like protein that is secreted by the neurons at the ventral midline of the animal (Ishii *et al,* 1992) and it acts as an attractant to UNC-40 (Chan *et al,* 1996*)* but a repellent for UNC-5 expressing growth-cones (Leung-Hagesteijn *et al,* 1992) (Figure 1.2.1). The function of UNC-6 seems to be conserved in higher organisms such as humans where its homolog, which is called netrin, also acts as a guidance cue for certain neuronal network formation and cell signalling (Serafini *et al*, 1994). Both UNC-5 (UNC-5a to UNC-5d in vertebrates) and UNC-40 (Deleted in Colorectal Cancer or DCC in vertebrates, Frazzled in *Drosophila*) are receptors which are expressed on actively migrating growth-cones. These receptors help detect ligand molecules like UNC-6 and steer the growth-cone appropriately (Colavita, 1998).

An additional guidance cue involved in dorsal migrations of cells and axons called UNC-129/TGFβ was found by Colavita et al., (1998). This cue is secreted from dorsal muscle and it is believed to attract axons towards the source of the cue. However, its exact function was unclear until recently.

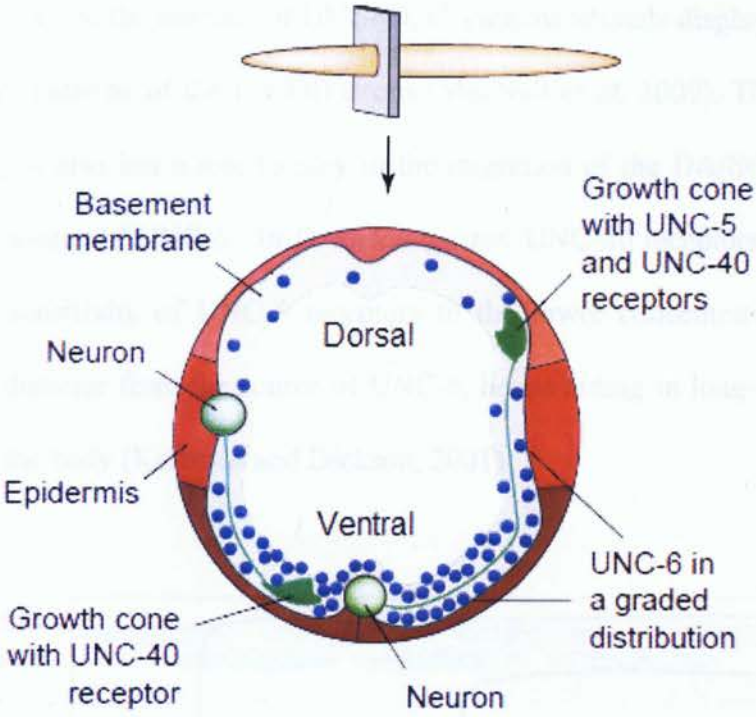

Figure 1.2.1: Patterns of migration for growth-cones expressing UNC-5 and UNC-40 receptors in a gradient of UNC-6 ligand molecules. Growth-cones expressing UNC-40 alone are chemo-attracted towards the ventral source of UNC-6 while growth-cones expressing both UNC-40 and UNC-5 are chemo-repelled away from the ventral source of UNC-6 (Wadsworth, 2002).

More recently, studies have shed light on the long-range repulsion mechanics of the *unc-5/unc-6* pathway (Figure 1.2.2). As UNC-5 expressing axons move away from the source of UNC-6, they encounter less and less of the UNC-6 ligand. Guiding these axons further towards the dorsal surface would require an additional cue or additional receptors that are sensitive to low concentrations of UNC-6. In the DA/DB motor neurons, both the UNC-5 and the UNC-40 receptors are expressed on the growth-cones which lead to the belief that UNC-5 overcomes the attraction of UNC-40 towards the source of UNC-6 (MacNeil *et*

al, 2009). However, in the absence of UNC-40, *C. elegans* animals display a slight defect in the migratory patterns of the DA/DB axons (MacNeil *et al*, 2009). This supports the idea that UNC-40 also has a role to play in the migration of the DA/DB growth-cones away from the source of UNC-6. In *D. melanogaster,* UNC-40 receptors are needed for increasing the sensitivity of UNC-5 receptors to the lower concentrations of UNC-6 found at some distance from the source of UNC-6, hence aiding in long-range guidance of axons along the body (Keleman and Dickson, 2001).

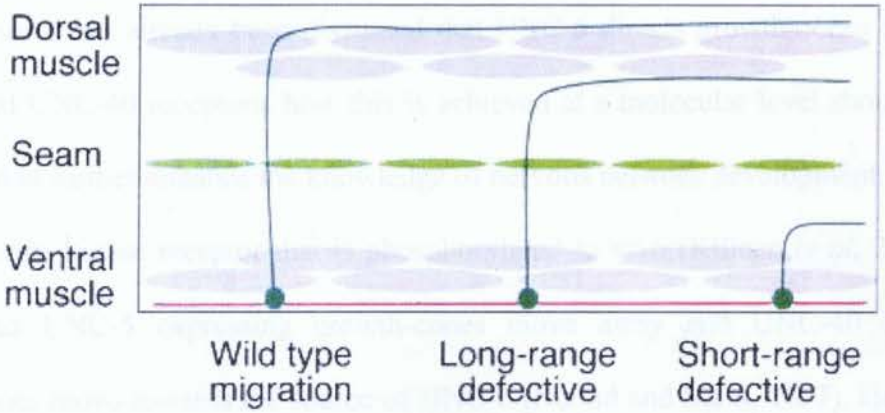

Figure 1.2.2: Degree of defectiveness in axon migration patterns shown according to where the seam of the animal is located. Short-range migrations of the DA/DB motor neuron axons are defective when either the UNC-5 receptor or UNC-6 ligand molecules are non-functional while long-range migrations of the DA/DB axons are defective if the UNC-40 receptors or UNC-129/TGFβ ligand are non-functional (MacNeil *et al*, 2009.

Mutants of the *unc-129* gene exhibit long-range defects in axon migration which suggested that UNC-129 plays a role in sensitizing UNC-5 receptors to low concentrations of UNC-6 (Colavita and Culotti, 1998). This idea was further supported

when *unc-129* and *unc-5* double mutants showed no greater enhancement of guidance defects compared to *unc-5* only mutants (MacNeil, 2009). Moreover, *unc-129* and *unc-40* double mutants did not show enhanced axon guidance defects compared to *unc-40* mutants alone (MacNeil, 2009). Both of these results suggest that *unc-129* is useful in long-range motor neuron axon guidance and also that it works in the UNC-5 + UNC-40 pathway by increasing sensitivity of UNC-5 to UNC-6 ligands.

1.3 Model for UNC-6/Netrin guidance of active axonal migration

Since it has already been discussed that UNC-6 directs growth-cones expressing UNC-5 and UNC-40 receptors, how this is achieved at a molecular level should also be understood to further enhance the knowledge of nervous network development. UNC-5 is a non-tyrosine kinase receptor that is phosphorylated in vivo (Killeen *et al*, 2002). It is known that UNC-5 expressing growth-cones move away and UNC-40 expressing growth-cones move towards the source of UNC-6 (Round and Stein, 2007). However, in the case of DA/DB motor neurons, both UNC-5 and UNC-40 receptors are expressed on growth-cones. Studies have shown that UNC-5 has an UNC-40 binding site called the DCC Binding (DB) motif which binds UNC-40 receptors and is essential for UNC-5 mediated repulsion in the DA/DB neurons (Round and Stein, 2007). Therefore, it should be understood that the presence of UNC-5 is dominant over UNC-40 when it comes to a decision on whether a growth-cone will move towards or away from the source of UNC-6 (Figure 1.3.1). It was shown recently that UNC-129/TGFβ disrupts the formation of UNC-5 homodimers and causes the formation of UNC-5 + UNC-40 heterodimers (MacNeil *et al*, 2009).

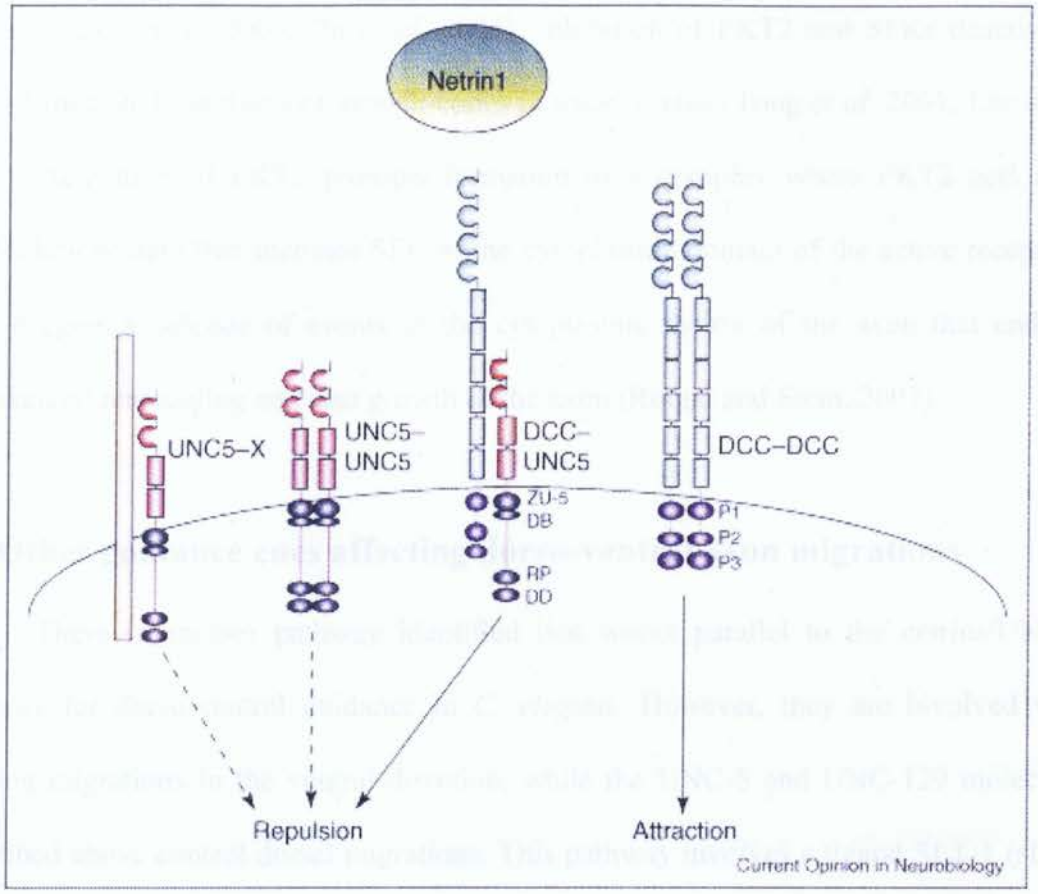

Figure 1.3.1: Signals induced at the growth-cone based on which combination of receptors are present on the surface and are binding to the UNC-6/Netrin ligand molecules. DCC/UNC-40 has three highly conserved repeats in the cytoplasmic domain called the P1, P2, and P3. P1 is essential for interaction with UNC-5 whereas P2 and P3 are useful in creating multimers with other DCC/UNC-40 receptor molecules. In UNC-5, the intracellular domain contains a zona occludens (ZU-5), a DCC binding site (DB), a repulsive motif, and a death domain (Round and Stein, 2007).

Other molecules are also implicated in working in concert with the UNC-6/netrin pathway and their receptors to trigger growth-cone response to UNC-6 signalling. These molecules are protein tyrosine kinase 2 (PKT2), Src-family Kinases (SFKs), and Rho

GTPases (Lee *et al,* 2005; Jin *et al*, 2005). Inhibition of PKT2 and SFKs deactivates UNC-5 mediated repulsion of growth-cones in mice *in vivo* (Tong *et al*, 2001; Lee *et al*, 2005). Activation of PKT2 prompts formation of a complex where PKT2 acts as a scaffolding protein that includes SFK at the cytoplasmic domain of the active receptors. This triggers a cascade of events in the cytoplasmic matrix of the axon that ends in cytoskeletal remodeling and also growth of the axon (Round and Stein, 2007).

1.4 Other guidance cues affecting dorso-ventral axon migrations

There is another pathway identified that works parallel to the netrins/UNC-6 pathway for dorso-ventral guidance in *C. elegans*. However, they are involved with guiding migrations in the ventral direction, while the UNC-5 and UNC-129 molecules described above control dorsal migrations. This pathway involves a ligand SLT-1 (slit in *D. melanogaster*) and its receptor SAX-3 (Robo in *D. melanogaster*) (Hao *et al*, 2001). These two proteins were discovered in *D. melanogaster* and were implicated in regulating axon migration through the commissural space of the fly brain (Hao *et al*, 2001). In worms, SLT-1 is expressed in the dorsal muscles and regulates migration of growth-cones expressing SAX-3 receptors (Figure 1.4.1) (Hao *et al*, 2001). This regulation is chemo-repulsive, as growth-cones expressing SAX-3 move towards the ventral side of the animal (Hao *et al*, 2001). One example of such neurons are the Anterior Ventral Mechanosensory neurons (AVMs) which are neurons whose cell bodies are located close to the mid-body region that send axons ventrally under the influence of SLT-1 ligands (Figure 1.4.1). Once the ventral cord is reached, the axons migrate in the anterior direction towards the head of the animal. Chemo-repulsion between SAX-3 and

SLT-1 was proven when SLT-1 was expressed symmetrically at the dorsal and the ventral side of the animal (Hao *et al*, 2001). In this case up to 70% of AVM axons failed to migrate towards the ventral cord and only went in the ventral direction. According to site-directed mutagenesis studies, the second Long Terminal Repeat (LTR) motif in SLT-1 is the essential component in ventral guidance of AVM axon (Hao *et al*, 2001). Also, in the absence of the SLT-1 receptor, SAX-3, the axons failed to move in the ventral direction and only moved towards the head.

The AVMs also failed to make ventral migrations in *unc-6* or *unc-40* mutants which suggest that both SLT-1/SAX-3 and UNC-6/UNC-40 pathways act parallel to each other and both are required for normal ventral migration of AVM axons (Hao *et al*, 2001). However, Slit and UNC-6 have opposing effects, since UNC-6 attracts the axons working through UNC-40/DCC and Slit-1 repels the axons working through SAX-3/Robo (reviewed by Killeen and Sybingco 2008). In order to further validate this result, double mutants of *slt-1* and *unc-6* or *unc-40* displayed 90% defects in guidance of the AVM axons in the ventral direction (Hao *et al*, 2001).

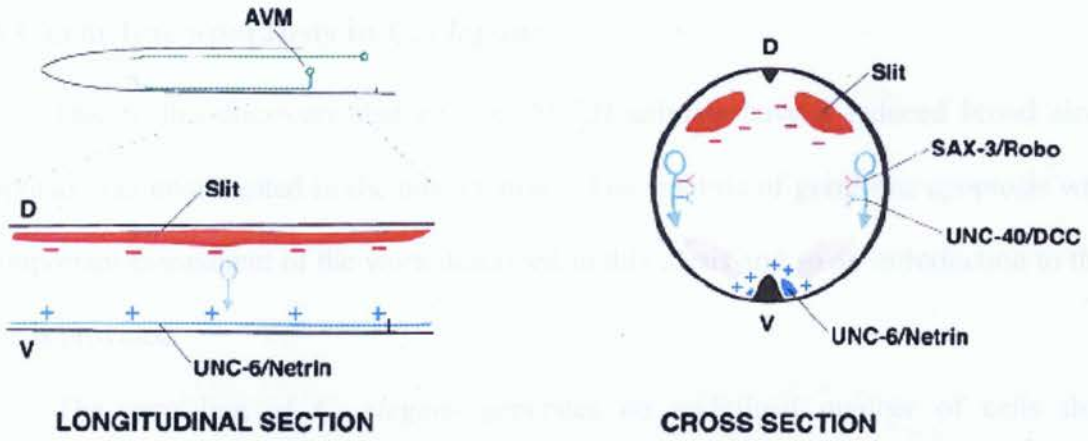

Figure 1.4.1: AVM neurons send out axons towards the ventral side due to chemo-repulsion (-) from SLT-1working through SAX-3 and also due to chemo-attraction (+) of UNC-6/netrin working through the UNC-40/DCC receptor (Hao *et al*, 2001)

The movement of AVM axons towards the anterior rather than the ventral direction in *sax-3* mutants indicates that axons recognize cues that lead them in the anterior-posterior (AP) direction indicating that SAX-3 is not responsible for AP guidance in the head region, i.e. short-range AP guidance. However, in earlier studies, it was found that SAX-3 is required for long-range AP guidance (Zallen *et al,* 1999) but this type of guidance is not required for sensory neurons like AVM neurons that are extending into the head region.

1.5 Germ-line apoptosis in *C. elegans*

Due to the discovery that *rq1;unc-5(e53)* animals have a reduced brood size, apoptosis was investigated in the mutant strain. The analysis of germ-line apoptosis was an important component of the work described in this thesis and so an introduction to the topic is provided.

The germ-line of *C. elegans* generates an undefined number of cells that proliferate until they become mature oocytes in the proximal end of the gonad. The gonad spans two thirds of the body of the worm and consists of two long tubes that start off at the ventral midline, go both in the anterior and the posterior directions away from the vulva, and then recoil back toward the dorsal midline making a symmetrical U shaped structure which is joined at the uterus (Figure 1.5.1) (Gumienny *et al*, 1999).

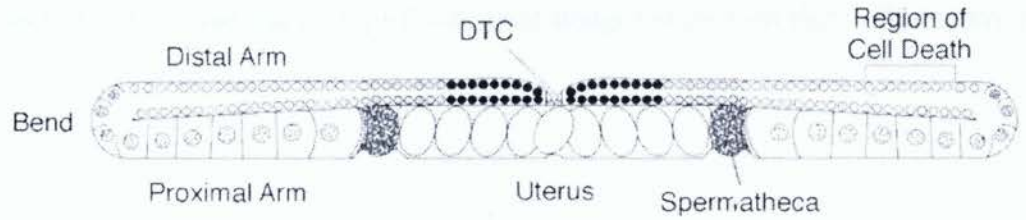

Figure 1.5.1: *C. elegans* gonad spans 2/3 of the worm body and encompasses the developing sperm and cells that become oocytes. Apoptosis of nuclei occur in the 'Region of Death' which is also known as the 'pachytene region' (Gumienny *et al*, 1999)

The Distal Tip Cell (DTC) is a somatic cell at the leading edge of the migration gonad arm which releases a signal called LAG-2. This signal keeps the stem cells dividing mitotically in the region indicated by dark spots beside the DTC (Guminney *et al*, 1999). The grey region marks the meiotically dividing germ cells which later enter the transition

zone or the region of cell death, also called the pachytene region. In this last region, germ nuclei which are fated to die undergo apoptosis by condensing their DNA material and swell up which can be visualized by Differential Interference Contrast (DIC) (Figure 1.5.2) (Guminney *et al*, 1999).

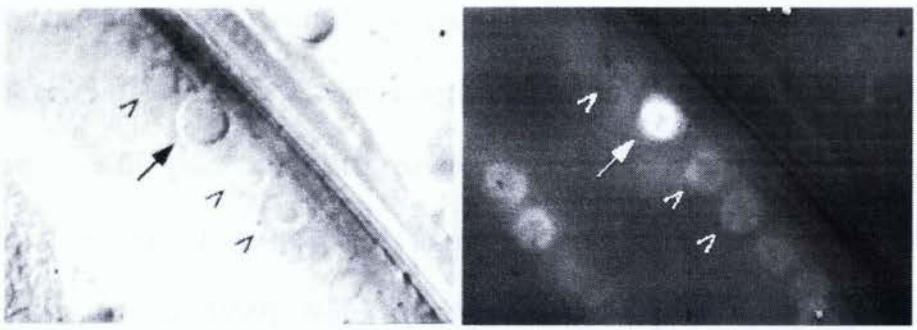

Figure 1.5.2: (Left) DIC image showing an apoptotic germ cell (large arrow). Normal nuclei are indicated by small arrows. (Right) Acridine Orange (AO) stains the apoptotic nucleus but not normal nuclei (epi-fluorescent image) shown on right (Gumienny *et al*, 1999).

Since the nuclei in the pachytene region are not surrounded by a cell membrane and share a common cytoplasm, it is hypothesized that the dying cells serve as nurse cells by providing essential nutrients like DNA material for the cells which are fated to live (Guminney *et al*, 1999). Moreover, when these dying cells were analyzed using the electron microscope, it was revealed that these cells isolated themselves from their neighbours by forming a plasma membrane around them that contained a small amount of cytoplasm. These cells are recognized and engulfed by gonadal sheath cells which form the lining of the gonad (Guminney *et al*, 1999).

Germ-line apoptosis starts when hermaphrodite animals are in the young-adult stage and oogenesis has started to take place. This idea was first hypothesized because there was no apoptosis that occurred in males and young larvae of either sex (Guminney *et al*, 1999). To test this hypothesis, *sdc-1* and *tra-1* mutants, which have oogenesis arrest and masculinization of the gonad producing only sperm, displayed no germ-line apoptosis. Therefore, it is assumed that physiological germ-line apoptosis is triggered only by the onset of oogenesis (Gummienny *et al*, 1999).

Exit from the pachytene zone requires the germ cells to activate the ras/MAPK signaling cascade that allows these cells to morph into oocytes and enter the fertilization zone (Gumienny *et al*, 1999). Normally, the ras/MAPK pathway is required for cell survival as indicated by previous studies in human carcinoma cell lines (Johnson and Lapadat, 2002), however, in the germline of *C. elegans*, this pathway is directly or indirectly required for the initiation of apoptosis. In mutants where this ras/MAPK pathway is blocked, germ-line apoptosis is also blocked. However, if double mutants were made with an apoptotic suppressor gene *ced-9*, apoptosis was initiated once again suggesting that ras/MAPK signaling could turn off *ced-9* which triggers programmed cell death in the germline (Gumienny *et al*, 1999).

1.6 Genetic pathways that trigger germline apoptosis

Altogether, there are more than 20 genes that have been identified as being responsible for germ-line apoptosis. Among these genes, 3 genes make up the 'core apoptotic machinery' that triggers apoptosis in both somatic and germ-line cells. These genes are *ced-3*, *ced-4*, and *ced-9* (ced is for Cell Death abnormal). Out of these three

genes, *ced-9* has a protective affect on the cell because it has been shown that *ced-9* mutants have an increased number of cell corpses present in the gonad. Both *ced-3* and *ced-4* genes are required for germ-line and also for somatic apoptosis as very little or no programmed cell death was observed in either of the mutants. Therefore, the core pathway looks like the one shown in Figure 1.6.1.

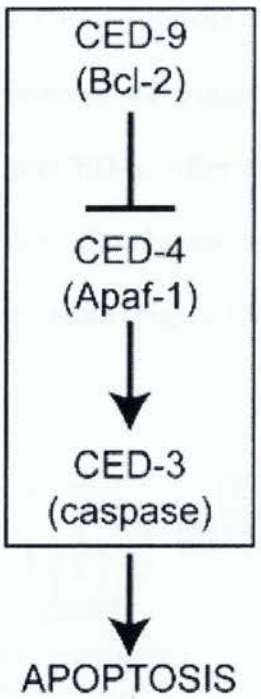

Figure 1.6.1: 'Core apoptotic machinery' indicating the three main apoptotic genes and their vertebrate homologues (Hengartner *et al*, 2006)

In mammals, Bcl-2 is homologous to CED-9 as it is an anti-apoptotic protein that contains four homologous Bcl Homomlogy (BH) domains. Apaf-1 (Apoptosis Protease Activating Factor – 1) is correctly identified as a homologue for CED-4 but CED-3

homologues remain very elusive as it matches a number of caspases in vertebrates (Hengartner *et al*, 2006).

When the ras/MAPK pathway is inactive, there is no physiological apoptosis taking place in the gonad. This inactivation of the core apoptotic machinery takes place when tetrameric CED-4 is broken up into dimers that are bound to CED-9 proteins at the surface of the mitochondria. In order to cause death in cells, CED-9 is inactivated by pro-apoptotic stimuli which releases CED-4 dimers that later form CED-4 tetramers (Hengartner *et al*, 2006). CED-3 proteins are proteolytically cleaved to activate CED-4 tetramers from a precursor called proCED-3. After cleavage, CED-3 forms an oligomer with CED-4 that is known as the '*C. elegans* apoptosome' which later activates downstream caspases and causes cell death (Figure 1.6.2) (Hengartner *et al*, 2006).

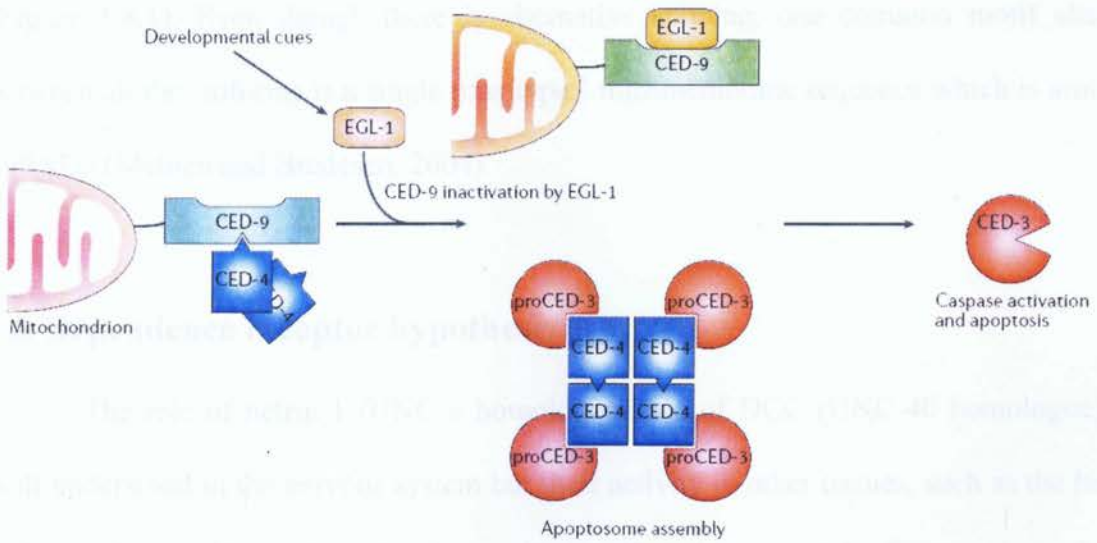

Figure 1.6.2: Pathway showing complex formation of 'core apoptotic machinery' due to activation of a pro-apoptotic protein called EGL-1 (Hengartner *et al*, 2006).

1.7 Genes involved in nervous system development induce apoptosis

As mentioned before, several apoptotic stimuli and program cell death inactivating factors are present inside and around the germ-line that control when and where apoptosis should take place. It has been shown that among these factors are genes that are known to play a role in nervous system development. The three genes that will be discussed here are the *unc-5*/Unc5, *unc-6*/Netrin, and *unc-40*/DCC whose role in nervous system development is well known and has been documented but whose involvement in apoptosis is somewhat controversial. Apoptotic roles of these genes have been analyzed in mammalian cell lines (Mazelin *et al,* 2004) but never before in *C. elegans*.

In humans, DCC is located on chromosome 18q on a region that spans a gigantic 1.2Mb region (Mehlen and Bredesen, 2004). The gene has more than 18 exons which produce several isoforms specific for different tissues including the nervous system (Figure 1.8.1). Even though there is alternative splicing, one common motif shared between all the isoforms is a single pass type I transmembrane sequence which is around 190 kDa (Mehlen and Bredesen, 2004).

1.8 Dependence receptor hypothesis

The role of netrin-1 (UNC-6 homologue) and of DCC (UNC-40 homologue) is well understood in the nervous system but their activity in other tissues, such as the heart and intestines, still needs to be thoroughly studied. My research shows a test of the dependence receptor hypothesis in the gonad of C. elegans where apoptosis has not been reported to be affected in the Netrin/UNC-6 pathway mutants.

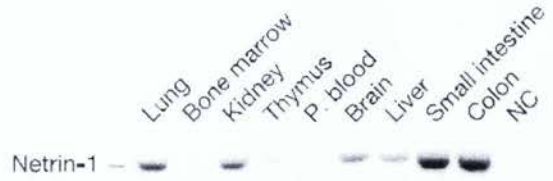

Figure 1.8.1: Western blot on protein extracts from various human tissue types indicating relative netrin-1 concentration present at specific time points (Mazelin *et al*, 2004).

In the mammalian small-intestine, Netrin-1 is most abundantly present at the base of the mucosal glands also known as crypts (Mehlen and Bredesen, 2004). Basal stem cells that express DCC on their membranes seem to differentiate in the crypt where Netrin signaling is abundant. As these cells move up the crypt, Netrin-1 concentration decreases and, it is hypothesized that, DCC triggers apoptosis when it cannot detect Netrin-1 ligands (Figure 1.8.2) (Mehlen and Bredesen, 2004). This conditional behavior of DCC would categorize it as a dependence receptor which is dependent on a ligand, in this case, Netrin-1, for preventing apoptosis and upon disengaging from Netrin-1, it triggers apoptosis.

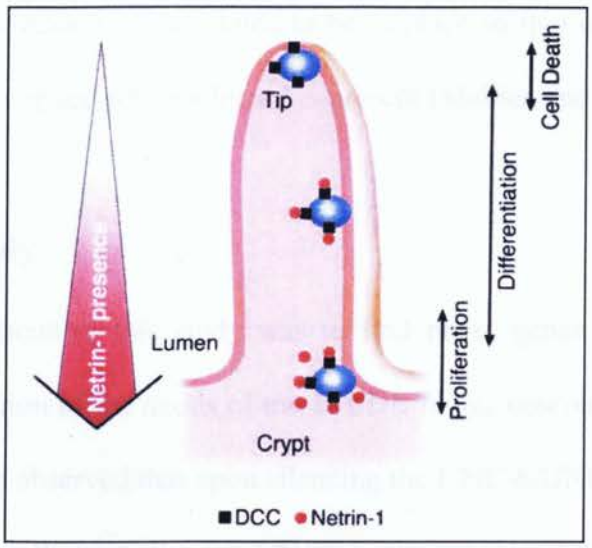

Figure 1.8.2: Image indicating zones of proliferation and differentiation of basal stem cells. Cell death occurs when these cells reach the tip of the crypt where netrin-1 concentration is very low (Mehlen and Bredesen, 2004).

To test the dependence receptor hypothesis, several experiments were conducted to investigate and validate netrin-1 and DCC interactions in the crypt (Mazelin *et al*, 2004). Firstly, transgenic mice (Tg-netrin-1) were created that over-expressed netrin-1. The mice grew and developed normally and when the crypts in the colon were examined for programmed cell death, it was noted that there was a 50% decrease in basal stem cell apoptosis. This was in-line with the dependence receptor hypothesis. Over-expression of netrin-1 was shown to result in an increase in colorectal tumors in Tg-netrin-1 mice and it was observed that 17% of the mice had at least one tumor in their intestine while the control displayed no tumor activity in the colon (Mazelin *et al*, 2004).

The protein UNC5H was also included in this dependence receptor category but its effects are not as predominant as they are for the DCC receptor. Several other proteins, such as Neogenin and Sonic Hedgehog receptor 'Patched' are also included in

this class and this mechanism is speculated to be in place so that cell proliferation does not take place beyond a space where a ligand is present (Mehlen and Bredesen, 2004).

1.9 Purpose of study

The primary focus of this study was to find novel genes that are involved in regulating axon migration of the axons of the DA/DB motor neurons. This idea was first developed when it was observed that upon silencing the UNC-6/UNC-5 pathway in either an *unc-6* or an *unc-5* null strain, the DA/DB motor axons migrated dorsally about two-thirds of the way towards the dorsal surface (Hedgecock *et al,* 1990). Since UNC-5 was the only receptor that was known to guide migrating growth-cones away from the source of UNC-6, this observation initiated the hypothesis that there must be other unknown proteins involved in axon migration. In an effort to identify genes in a pathway parallel to the *unc-6/unc-5* pathway genetic enhancer screens were performed to identify mutants that enhance the defects of *unc-5(e53)* mutants. One of these mutants was the allele *rq1*. The current study was mainly directed towards identification of the gene altered in the *rq1* allele.

The main reason for the analysis of apoptosis described in this study is that the *rq1* mutant, isolated as an enhancer of the axon outgrowth defects of *unc-5(e53)* was also found to have a very low brood size. One explanation for the low brood size would be increased levels of gonadal apoptosis. If apoptosis was altered in the germ-line it would support the hypothesis that genes that are involved in nervous system development could also be involved in regulating apoptosis as it was shown with Netrin-1, DCC, and UNC-5H in the dependence receptor hypothesis.

1.10 Genetic enhancer screen

A genetic enhancer screen was performed to observe if the defects that were already present in an *unc-5(e53)* mutant (considered to be a null mutant) could be made more defective by randomly creating mutations and screening for a specific defect, in this case axon outgrowth defects. The starting strain that was used in this screen was *unc-5(e53)* which is a null allele for *unc-5* (Hedgecock et al, 1990; Killeen *et al,* 2002). An *unc-129::gfp* gene was integrated in this strain to serve as a marker for the DA/DB neurons as UNC-129 is specifically expressed in these two neuronal classes (Colavita *et al*, 1998). Worms that had not started to lay eggs, L4 stage worms, were soaked in Ethyl Methane Sulfonate (EMS) to ensure that mutations take place in the growing nuclei inside the gonad. EMS randomly makes Guanine to Adenine mutations in *C. elegans* (Figure 1.10.1) (Hope, 1999). This procedure is also described in Materials and Methods.

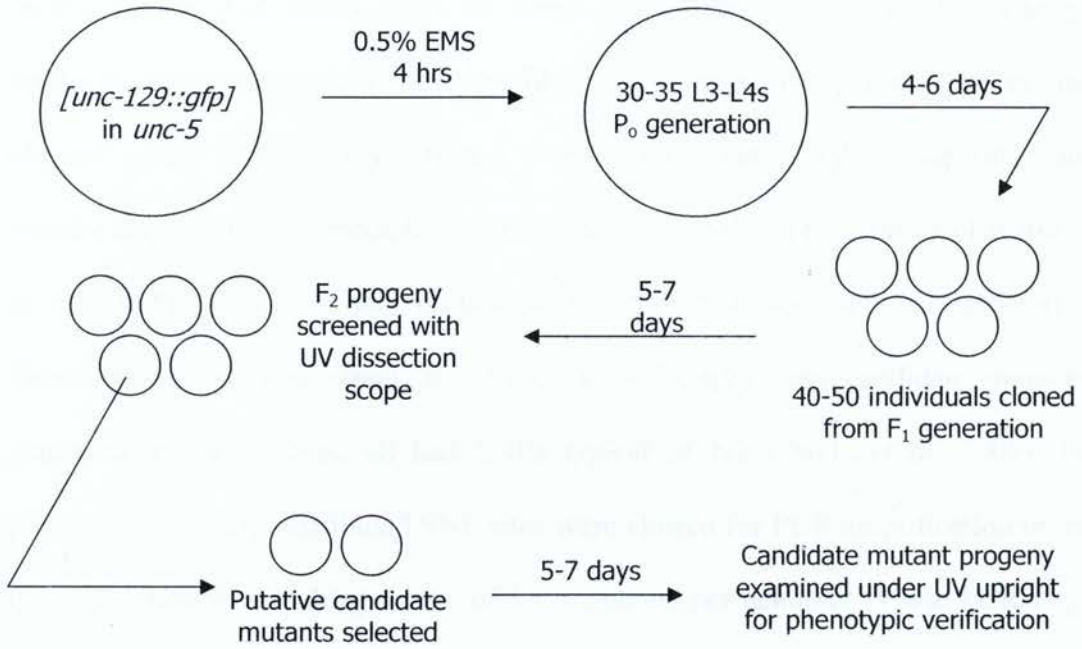

Figure 1.10.1: Genetic enhancer screen in *C. elegans*. Screening for enhancement of axon guidance defects was done in F2 progeny because mutations created by EMS were likely to be recessive and would only display a mutant phenotype when present in a homozygous arrangement (Sybingco, MSc Thesis, 2008).

Once there were candidates from the screen, they were out-crossed with the starting strain for isolation of the target gene. Out-crossing with starting strain eliminates unlinked background mutations as the F2 progeny of the cross displays a mixed progeny due to recombination in meiosis 1 (Davis *et al*, 2005). This mixed progeny was then screened for worms that display the enhanced axon guidance defects seen in the original mutant. The out-crossing procedure is repeated several times to ensure isolation of the target gene in order to eliminate any other unlinked mutations caused by the mutagen besides axon guidance defects.

Candidate genes were mapped on *C. elegans* genome by a method called the snip-SNP method (Davis *et al*, 2005). SNPs are Single Nucleotide Polymorphisms that are present on the *C. elegans* genome and are specific to each strain in a species. Two strains in *C. elegans* would have slightly different SNP locations compared to each other and this became the underlying principle on which the snip-SNP mapping protocol works (Davis *et al*, 2005). Mutant strains in this study originated from the N2 (Bristol) strain. Therefore, the starting strain, *unc-5(e53)[unc-129::gfp]*, and candidate mutants with enhanced axonal defects, all had SNPs typical of N2 (Davis *et al*, 2005). For the procedure, 8 evenly distributed SNP sites were chosen for PCR amplification on each of the 6 chromosomes making a total of 18 fragments per genome. These PCR fragments when digested by the DraI restriction enzyme give bands characteristic of N2 but different from the related Hawaiian strain. Given that the SNPs are evenly distributed along chromosomes, mutations in genes of interest would be closely linked to certain N2 SNPs on one chromosome but not to most others (Figure 1.10.2) (Davis *et al*, 2005).

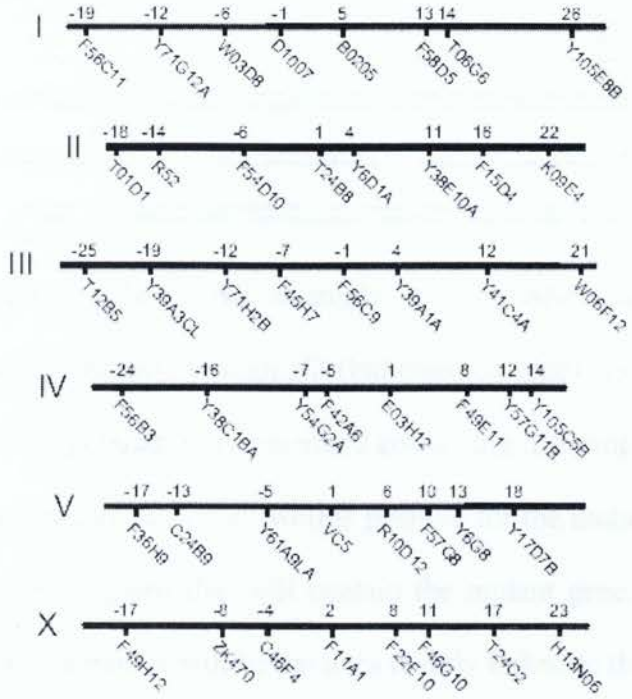

Figure 1.10.2: N2 SNP sites selected for their ability to be digested by DraI. Roman numerals refer to Chromosome numbers except for 'X' which shows SNP sites on the X Chromosome (Davis *et al*, 2005). The primers used in this study were described by Sybingco (MSc thesis York University 2008).

The mutant strain was crossed with a Hawaiian (CB4856) strain with different SNP locations where this cross gives heterozygous F1 progeny containing both N2 and Hawaiian chromosomes. In the F2 generation, a mixed population is generated which has worms that are homozygous for axon guidance mutations and display this phenotype. Any worms displaying this phenotype are picked and categorized as positive for the mutation and those that do not display the phenotype are negative for the mutation. All worms that are positive for the mutation would have a section of the N2 genome that would carry the mutant gene and the closely linked SNPs on it (Davis *et al*, 2005).

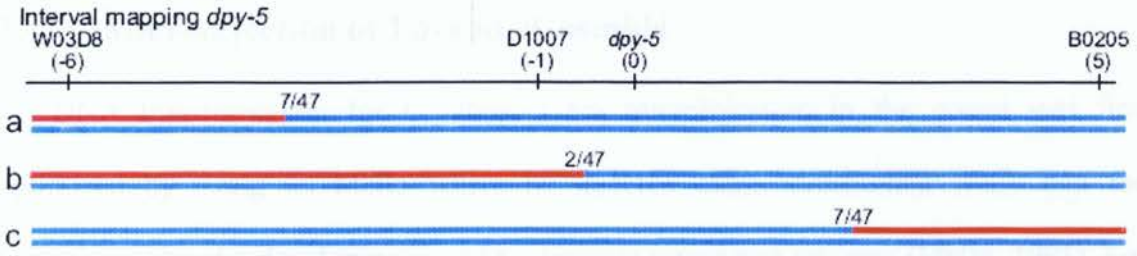

Figure 1.10.3: An example of snip-SNP mapping using *dpy-5* gene. During recombination between N2 (indicated by blue) and Hawaiian (indicated by red) strain, a mixed population is generated containing differing lengths of chromosomal segments of each strain. However, worms positive for the mutant phenotype will be homozygous for the N2 regions that will contain the mutant gene. N2 SNPs that reoccur frequently in positive worms will be the ones closely linked to the mutant gene, in this case D1007 and B0205 (Davis *et al*, 2005). In the example shown there were 47 F2 animal pools tested and the numbers indicate the numbers that exhibited the linkage shown in the diagram.

Positive and negative pools of worms are then lysed to release DNA material that could be used in SNP directed PCR and the most *reoccurring* N2 SNPs could be identified for each positive worm. Theoretically a finding of 50% recombinants indicates no linkage between the gene and the SNP. The N2 SNP that reoccurs most of the time in mutant positive worms would be closely linked to the site of mutation and hence will have a decrease rate of recombination with the Hawaiian genome (Davis *et al*, 2005). Using this method, a mutation is narrowed down to a segment of the genome which could then be narrowed down further by subsequent snip-SNP mappings or microinjections of fosmids/cosmids containing wild-type DNA (Davis *et al*, 2005).

1.11 Microinjection of Fosmids/Cosmids

DNA transformation for *C. elegans* via microinjection in the gonad was first optimized by Craig C. Mello where he injected extrachromosomal DNA into the transition zone of a developing gonad to generate transgenic progeny (Mello, 1991). For this procedure, he used a semi-dominant right roller allele of a gene called *rol-6* which induces a helically twisted cuticle and body structure.

As seen in Figure 1.11.1, the centre core of a gonad is filled with cytoplasmic material that works as a syncytium which provides nourishment for the developing nuclei surrounding it. This cytoplasmic material is enclosed by a cell membrane around nuclei as they approach the bend of the gonad (Gumminey *et al,* 1999).

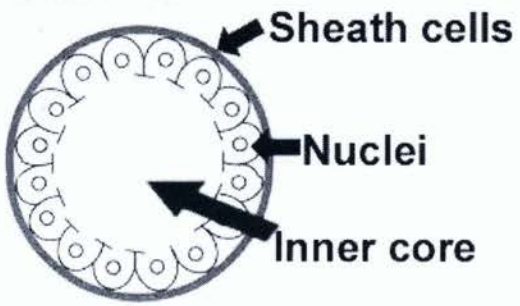

Figure 1.11.1: Cross-sectional view of *C. elegans* gonad. The inner core of a gonad is a syncytium made up of cytoplasmic material which is shared by all developing nuclei that surround it. Sheath cells isolate the gonad from rest of the inner organs and are responsible for other functions such as replenishing the inner core, discarding waste material, and engulfing abnormal germ-line cells that fail to develop (Gumminey *et al*, 1999).

Taking advantage of this structural setup and the large diameter of the inner gonad core, Craig Mello injected the pRF4 plasmid containing the *rol-6* mutant gene into wild-type animals obtaining around 20-50 transgenic animals in the progeny of each injected animal (Mello, 1991). Foreign DNA would be incorporated into a developing germ cell when it is enclosed by a part of the cytoplasm from the inner core which contains the injected DNA. Considering that each wild-type animal lays on average 250 eggs, the transformation efficiency for this technique lies somewhere in the range of 8-20% (Mello, 1991). The number of transgenics obtained in the progeny depended on the concentration of plasmid DNA that was used in microinjections. A 20% transformation rate was achieved when 200μg/ml of the plasmid was injected (Mello, 1991). As shown in Table 1.11.1, transformation efficiency did not increase significantly after 50μg/ml of plasmid DNA.

pRF4 (μg/ml)	Number Injected	F1 rollers		
		Total	Per injected animal	Maximum
12.5	11	78	7.1 ± 5.1	18
25	27	313	11.6 ± 6.6	27
50	15	398	26.6 ± 10.8	56
100	20	498	24.9 ± 9.5	45
200	14	400	28.6 ± 8.4	50

Table 1.11.1: Data showing effect of plasmid DNA concentration on efficiency of transformation in wild-type animals. The maximum increase can be seen when the concentration was increased from 25μg/ml to 50μg/ml. This indicates that plasmid DNA concentrations above 50μg/ml will generate a viable number of transgenic animals (Mello, 1991).

1.12 Goal of current thesis work

The main focus of my thesis work was related to *rq1*, a mutant in *unc-5(e53)[unc-129::gfp + dpy-20]* strain, which was isolated as a genetic enhancer in the screen described above. The mutation was mapped down to the 2.126 to 3.923 region of chromosome III which contains 88 genes (Sybingco, M.Sc Thesis, 2008). In an attempt to further narrow down the mutant gene region, microinjection of eight overlapping cosmids/fosmids containing wild-type copies of 88 genes were injected to identify the gene that would rescue the axon outgrowth defect phenotype in *rq1;unc-5(e53)* (Bueno de Mesquita MSc Thesis, Ryerson 2008). This work identified a rescuing fosmid called H04D03 which contained the genomic version of 6 genes namely M03C11.8, H04D03.1, H04D03.2, H04D03.3, H04D03.4, H04D03.5. ***The primary goal of this study was to confirm that H04D03 was indeed the fosmid that rescued the defects of the mutant rq1. If this was proven, the correct gene from the fosmid had to be identified. Furthermore, mutant phenotypes besides axon guidance defects were also analyzed and are presented in this study.***

2.0 Materials and Methods

The following materials and methods were used during the course of this project. References are provided for each method for more detailed explanation.

2.1 Strains used in study

The DA/DB motor neurons and their axons were visualized by use of a transgenic GFP under the control of the *unc-129* (UNC for UNCoordinated) neuronal promoter (Colavita *et al.* 1998). This strain contains the neuronally expressed *unc-129* promoter with *dpy-20* and the integrated line is called *[evIs82B]*. Strains used were *unc-40(e1430)* Linkage Group (LG) I, *rq1*: LG III, *unc-5(e53)* LG IV, *unc-6(ev400),* LG X, Strains made using this transgene were *unc-5(e53)[unc-129::gfp], unc-6(ev400)[unc-129::gfp], unc-40(e1430)[unc-129::gfp]*. These strains were obtained from Dr. Joseph Culloti's lab at Mount Sinai Hospital.

A screen for axon guidance mutants was conducted in an *unc-5(e53)* genetic background and several alleles were found and mapped on the genome (Sybingco, M.Sc. thesis, 2008). These mutants all enhance the axon guidance defects of *unc-5(e53)* considered to be a null mutant of *unc-5* (Hedgecock *et al*, 1990, Killeen *et al*, 2002). Mutants from axon guidance screens are called by the allele name '*rq*' as this is the designation for the Killeen lab in the *C. elegans* community; hence the first mutant was termed *rq1*. Strains constructed containing *rq1* were *rq1*4[evIs82B], rq1*3;unc-5(e53);him-5[evIs82B], rq1*6;unc-6(ev400)[evIs82B], rq1*6;unc-40(e1430)[evIs82B]* where * indicates the number of outcrosses performed against a wild-type strain to eliminate unwanted mutations.

2.2 Preparing seeded NGM plates

Regular Nematode Growing Media (NGM) plates seeded with the OP50 strain of *E. coli* were used to maintain and cultivate worms at 20°C as directed in Brenner (1974). NGM plates were made using 3g/L NaCl, 2.5g/L Bacto peptone, 17g/L agar in deionized water. The solution was stirred for 2 minutes with a magnetic stir bar and placed in an autoclave for 70 minutes at 122°C. After autoclaving, the solution was stirred until it reached 55°C. 1ml of 5mg/ml cholesterol (in ethanol), 1ml of 1M $CaCl_2$, 1ml of 1M $MgCl_2$, and 25ml of 1M K_2PO_4 were added in this order while the solution was stirred until it was cool to touch. After pouring media into plates, these were left at room temperature and the medium inside was allowed to solidify. Plates were seeded using 1ml O/N culture of the OP50 strain of *E. coli* bacteria in LB diluted with 5ml of M9 (22mM KH_2PO_4, 22mM Na_2HPO_4, 85mM NaCl, 1mM $MgSO_4$) buffer (Hope *et al.* 1999). Plates were then incubated for 24hrs at room temperature and then placed in 4°C until use.

2.3 Quantification of axonal defects

Animals were placed on a 2% agarose pad on Fisher brand glass microscope slides with a drop of 1mM levamisole to prevent worms from moving (Brenner, 1974). DA/DB motor neurons fluoresced under the epifluorescent microscope due to the *unc-129::gfp* transgene which is a *gfp* gene under the control of the *unc-129* neuronal promotor. Since UNC-129 is only expressed in DA/DB motor neurons, the transgene expressed GFP only in these neurons as well. Axons which failed to exit the ventral nerve cord of animals were counted as defective in outgrowth.

2.4 EMS mutagenesis

unc-5(e53)[unc-129::gfp +dpy-20] strain was deposited onto two large plates and left to grow at 20°C until there were a substantial number of L4 or young adults on the plates (Sybingco, MSc Thesis, 2008). A 5ml aliquot of M9 was pipetted onto the worms on each plate to have animals float in solution. Plates were swirled for 20 seconds to obtain a large number of worms. M9 solution containing worms was then aspirated off from both plates with a pipette and the volume of solution was noted. The solution was pipetted into an empty large plate which was then placed in a fume-hood. Around 50-100µl of EMS solution was transferred into the plate containing worms in M9. The solution was left standing covered with a lid for 4 hrs in the fume-hood. Solution was transferred to a 15mL Falcon tube and spun in a centrifuge at 5000g for 20 seconds. Supernatant was discarded and the worm pellet was resuspended in 5ml of fresh M9. The tube was spun again and the supernatant was discarded. The M9 washing was done twice more to make sure that most of EMS was washed off the worms. After the last M9 wash, the worms were resuspended in 5mL M9 and transferred onto a medium seeded plate. The plate was left to dry for 60-90mins. Around 10-15 L4 or young adult animals were picked off this medium plate and placed onto a fresh medium seeded plate for two days. Next, these animals were transferred onto another fresh medium seeded plate for two more days. Around 20 non-Unc F1 animals were placed on individual small seeded plates and their progeny were screened for axons which fail to exit the ventral nerve cord. At this point the animals are in the F2 generation to allow mutations to homozygoze. Screens were done using a Leica dissection microscope, MZFLIII (Sybingco, MSc Thesis, 2008).

2.5 Apoptosis staining and counting

L4 animals were picked and placed to be staged on small plates to grow over a period of 24-48 hours. 150 µl of 0.05mg/ml acridine orange (AO) was transferred and spread onto small seeded NGM plates. These AO stained plates were kept in the dark for 24 hours. L4 stage or young adult worms were transferred onto stained plates for 1 hour after which they were transferred to a normal seeded plate for 2 hours to destain (Derry *et al*, 2008). These worms were transferred onto a drop of levamisole on 2% agarose pad slide and the pachytene area in posterior gonads were examined on a Leica (model DM5000B) for fluorescent nuclei using a mercury vapour UV light source and GFP filter in a low light situation to prevent fading of the AO.

2.6 Immuno-fluorescence staining of *C. elegans* embryos

Young adult hermaphrodites were picked and transferred into a drop of 150 mM KCl on a glass slide which was pre-coated with 0.1% poly-lysine. An insulin needle was used to dissect the worms at the midsection to release mature eggs. A coverslip was placed on top of these eggs and the slide was place on dry ice to promote freezing. After 20mins, the coverslip was removed with a sharp metal blade before the ice inside could melt. This freeze fracture procedure allowed the chitin shell to break open. The slide was then fixed in MeOH at 4°C for 10mins and then washed for 2 mins with Phosphate Buffer Saline (PBS) solution. The slide was then washed for 10 mins with PBS + 0.5% Tween-20 (PBST) and then blocked by PBS + 10% goat serum + 1% BSA (PBGS) for 30 mins at room temperature. A 1:100 dilution of secondary antibody (Wheat germ agglutinin -

fluorescein isothiocyanate or WGA-FITC) was applied to the sample for 2-4 hrs. No primary antibody was used because WGA-FITC binds directly to the α2-3 linked sailic acids in mammalian cells (Wendy Johnston *et al*, 2006).

Chitin staining was done with a chitin-binding probe (chitinase A1 chitin-binding domain fused to maltose binding protein and labeled with TRITC (CBD-F)). This probe was diluted in PBGS at a ratio of 1:250 and then applied to sample overnight. DNA was stained with Hoechst (Molecular Probes) stain and then SlowFade (Molecular Probes) was added to the sample before the sample was exposed to UV light.

2.7 Microinjection of cosmids/fosmids

Preparation of cosmid/fosmid DNA was done using a modified alkyline lysis method (Lin and Floros, 2000). DNA was electrophoresced on 0.7% agarose and its concentration was estimated by comparison to the nearest band in DNA ladder. A mix of *myo-2::yfp* (*yfp* under control of *myo-2* promoter) (Miller, 1986), which is the co-injectable marker, and the DNA of interest was made to a concentration of 50-100 μg/ml in water (3:7 ratio of co-injectable marker: plasmid DNA) to obtain optimal numbers of transgenic progeny (Mello, 1991). For routine experiments where F1 rescued animals were scored, 30 μg/ml of *myo-2::yfp* and 70 μg/ml of fosmid, cosmid or plasmid was used. For generation of stable lines, a concentration of 10 μg/ml of *myo-2::yfp* + 90 μg/ml of plasmid was found to be preferable. A 0.2 μl aliquot of this mix was transferred into a 0.75 mm glass needle (Olympus Inc.) which was pulled using a P-97 Flaming/Brown Micropipette Puller (Sutter Instrument Company). A needle was mounted onto a stylus and the tip was broken by touching it to the side of a coverslip.

Pressure of around 20 psi was applied to prevent clogging of the needle with glass fragments. The DNA mix was injected into young-adult mutant hermaphrodites as shown in Figure 2.6.1. These animals were in oil and were mounted upon a 1% agarose pad. After microinjection, hermaphrodites were placed onto a freshly seeded plate and were soaked in M9 solution. These animals were left to recover and were screened after 2-3 days for transgenic progeny (Bueno de-Mesquita, M.Sc. Thesis, 2008).

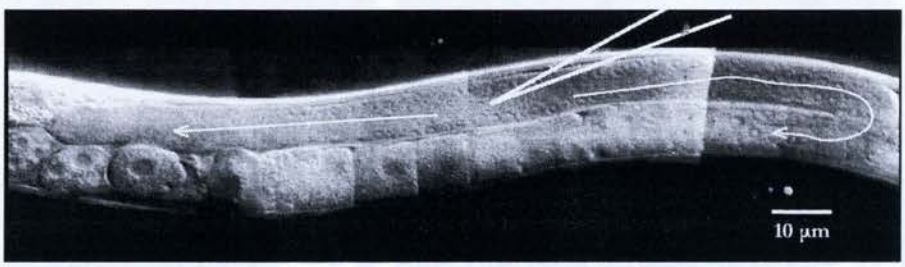

Figure 2.6.1: Microinjecting DNA mix into the distal end of young-adult hermaphrodite gonad (Mello, 1991).

myo-2p::yfp (Miller, 1986) was used as a co-injection marker and it was injected along with the DNA of interest into mutant animals. This construct contains the *myo-2* promoter driving YFP, so it is a transcriptional fusion. F1 animals expressing yellow fluorescent (YFP) protein in the pharynx were picked as transgenics These transgenics contain extrachromosomal arrays and few are passed onto the F2 generation. There is a slight overlap in fluorescence between the GFP and the YFP proteins when seen under the Leica MZFLIII dissection microscope under the GFP filter (Excitation filter 425-460nm, Barrier filter 480nm) but once the YFP filter (Excitation filter 510-520nm,

Barrier filter 540-560nm) is in place, background fluorescence decreases significantly leaving only the YFP in the pharynx visible (Figure 2.6.2).

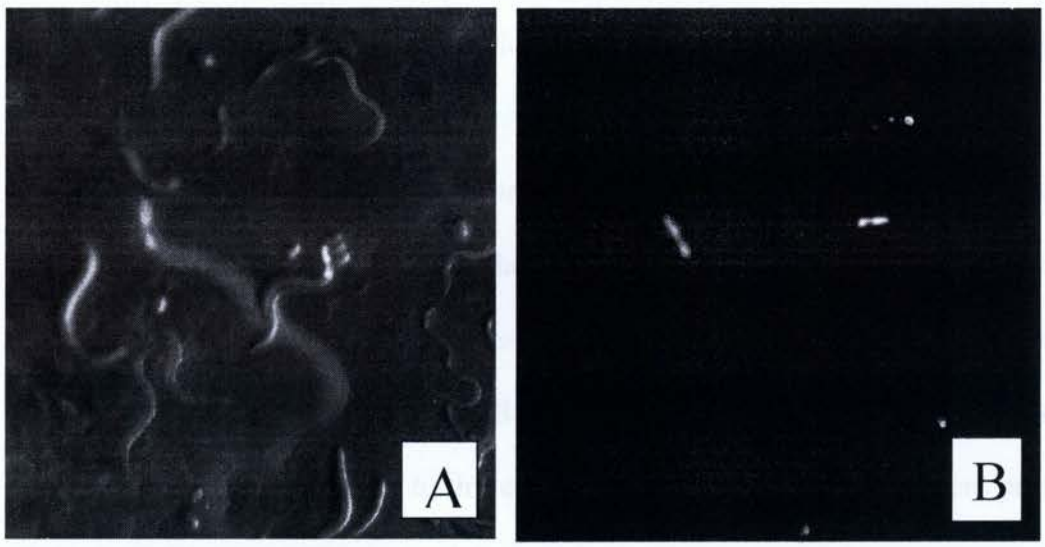

Figure 2.6.2: Worms microinjected with *myo-2::yfp* co-injectable marker. A) Mixed transgenic and non-transgenic progeny from microinjected animals under the GFP filter. B) Transgenic animals can be seen once YFP filter is in place. Worms with *myo-2::yfp* gene express YFP protein in pharyngeal muscles where myosin 2 heavy chain proteins are normally expressed (Miller, 1986).

3.0 Results

My research has focused on improving our understanding of nervous system development, in particular in understanding the guidance cues for migration of neuronal axons. Towards this end, we have made use of the model genetic organism, the microscopic nematode *C. elegans*, which has a simple nervous system consisting of only 302 neurons in the adult hemaphrodite.

For the current study, we focused on the axon guidance of a particular class of motor neurons called the DA and the DB motor neurons. DA/DB motor neurons are pioneer neurons whose axon processes are guided by the UNC-6/netrin pathway proteins (Hedgecock, *et al*, 1990). DA and DB motor neurons can be detected using the neuronal promoter of the *unc-129* gene to drive the expression of green fluorescent protein (GFP) (Colavita *et al*, 1998). The particular construct used contains an integrated copy of a wild-type copy of the *dpy-20* gene along with *unc-129::gfp* and it is known as evIs82B (Colavita et al., 1998). UNC-6 is a graded ligand expressed at the ventral midline of the animal (Ishii *et al*, 1992, Wadsworth *et al*, 1996) and UNC-5 is a receptor (Leung-Hagesteijn *et al*, 1992) which together with the UNC-40/DCC receptor (Chan et al., 1996) guides growth-cones towards the dorsal surface, away from the source of UNC-6. Axons migrating in the dorsal direction are also guided by attraction to UNC-129/TGFβ, expressed in dorsal muscle band (Colavita *et al*, 1998).

In *unc-6(ev400)* or *unc-5(e53)* mutants, the animals are very uncoordinated (Unc) since the migration of many motor neurons is altered (Hedgecock *et al*, 1990). These two strains are putative nulls and the mutant genes in both have been sequenced (Wadsworth *et al*, 1996; Killeen *et al*, 2002). In these genetic backgrounds the DA and DB motor neuron

axons leave the ventral cord as normal but migrate either 1/3 or 2/3 of the way towards the dorsal cord, never reaching their normal muscle targets (Hedgecock *et al*, 1990; Colavita *et al*, 1998) (Figure 3.0.1.B), whereas the axons migrate all the way to the dorsal cord in wild-type animals (3.0.1.A). In the absence of the UNC-5 receptor, the axons are still directed somewhat in the dorsal direction indicating that there are other proteins that guide these axons away from the ventral nerve-cord. Since these unknown proteins work in the absence of the UNC-5/UNC-6 pathway, it is assumed that they are working independently of this pathway. Screening for novel mutants that enhance the axon guidance defects of *unc-5(e53)* was performed and three novel mutants were found in a genetic enhancer screen done at Ryerson. The screen methodology is described in the introduction and previously by Sybingco (2008). The mutants found in the screen have defects in outgrowth of the axons form their cell bodies in the ventral cord. These outgrowth defects are observed in *unc-5(e53)* and *unc-6(ev400)* animals, but the numbers are increased in the new mutants found in the screen. Three mutants *rq1, rq2,* and *rq3* were identified in the screen and were mapped by snip-SNP mapping on the genome (Sybingco, 2008). *rq1* was mapped to LGIII, *rq2* to LG X and *rq3* mapped to LG IV. An animal from the *rq1* strain is shown in Fig.3.0.1C where many of the axons fail to exit the ventral cord.

The current study focuses on the *rq1* mutant phenotype. *rq1* alone primarily causes axon outgrowth defects of particular axons and also causes mild axon guidance defects on its own in an otherwise wild-type background. The main purpose of the current study was the identification of the gene that is implicated in causing these defects.

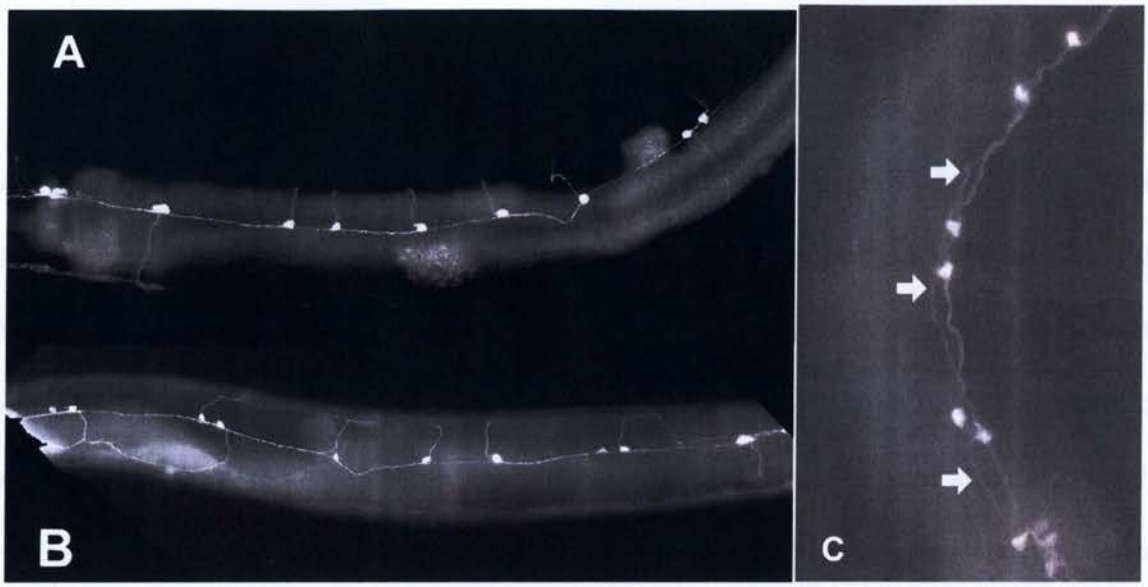

Figure 3.0.1: Images showing the DA and DB motor neuron axon outgrowth from cell bodies located in the ventral cord (View is of the ventral side of animals). The DA and DB motor neuron axons can be seen leaving their cell bodies in the ventral cord in a) in N2 [*unc-129::gfp + dpy-20]* b) *unc-5(e53)[unc-129::gfp + dyp-20]* strain and c) *rq1*3;unc-5(e53);him-5[unc-129::gfp + dyp-20].* Arrows in Figure c) indicate neuronal bodies missing axons completely and some that migrate along the ventral cord.

3.1 Axon guidance and outgrowth defects displayed by *rq1* mutants:

Worms that contain the *rq1* mutation in *unc-5(e53)* have enhanced DA/DB motor axon guidance and axon outgrowth defects compared to *unc-5(e53)* (Figure 3.1.1). When quantifying the number of defective axons, we were not concerned with long-range or short-range migration defects in axon migrations from the ventral cord, but rather with axons that failed to exit the ventral nerve-cord and these are called axon outgrowth defects. They could be axons that fail to grow out of their respective cell bodies or those

which go along the ventral nerve-cord but never migrate in the dorsal direction (Figure 3.0.1C).

The DA/DB axon outgrowth defects depend on the degree of penetrance of the *rq1* mutation which was found to be different when considering each of the 14 neurons (penetrance refers to the number of defective axons among a population). Axons near the head of worms were not scored, due to difficulty in identifying them separately from each other. Quantification was easier starting from the DA4 motor neuron up to those at the tail and among these neurons, only the DB neurons in the middle were affected by *rq1* while the DA motor neuron axons were essentially unchanged from their appearance in an *unc-5(e53)* background. The three most affected DB neurons were DB4, DB5, and DB6 (Figure 3.1.1). The original screen was done in *unc-5(e53)*, a putative null strain, so the outgrowth defects were quantified in this background (Figure 3.1.1). An increase of 25-35% in axon outgrowth defects in the double mutant *rq1* strains compared to the background strains suggests that *rq1* works independently of both *unc*-5 and *unc-6*. This result is satisfying as the screen was set up to find genes in a pathway parallel to the *unc-6/unc-5* genetic pathway.

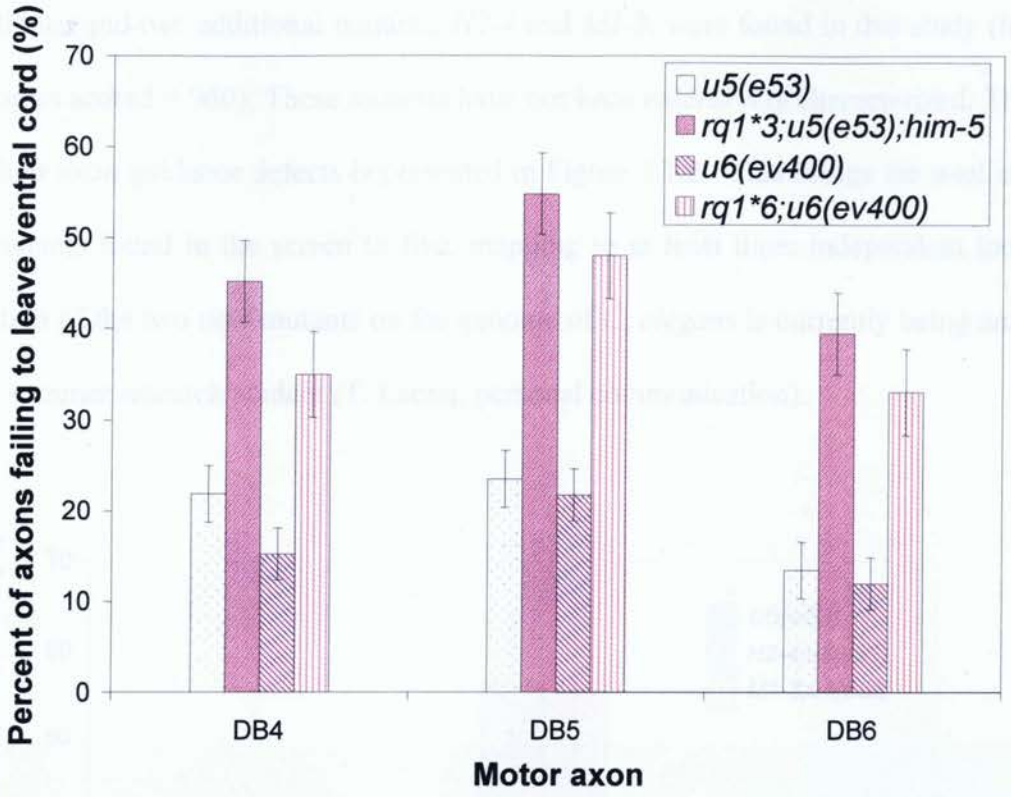

Figure 3.1.1: Graph showing a comparison between the *unc-5(e53)* and *unc-6(ev400)* null mutants and doubles with *rq1*. When an axon fails to exit the ventral cord it is recorded as a defect for that neuron. Each cell body is scored individually. Axon outgrowth defects for DB4, DB5 and DB6 in *unc-5(e53)[unc-129::gfp]* were scored and presented as stippled bars. The double mutant background of *rq1*3;unc-5(e53);him-5[unc-129::gfp]* is presented as small checked bars. The outgrowth defects were also quantified in the absence of the ligand UNC-6/netrin that binds the UNC-5 receptor. The outgrowth defects are presented for *unc-6(ev400)[unc-129::gfp]* in diagonal striped bars and the data for the *rq1*6:unc-6(ev400)[unc-129::gfp]* in vertical striped bars. Vertical error bars were calculated by using standard error of measurement in Microsoft™ Excel® 2007 (Hatch, Lazaraton, and Dudek model) (n = 120).

The genetic screen for enhancers of the axon guidance defects of *unc-5(e53)* was continued and two additional mutants, *H2-4* and *M1*-3, were found in this study (haploid genomes scored = 960). These mutants have not been extensively characterized. The data on their axon guidance defects is presented in Figure 3.1.2. This brings the total number of mutants found in the screen to five, mapping to at least three independent loci. The location of the two new mutants on the genome of *C. elegans* is currently being analyzed by a summer research student (T. Lacraj, personal communication).

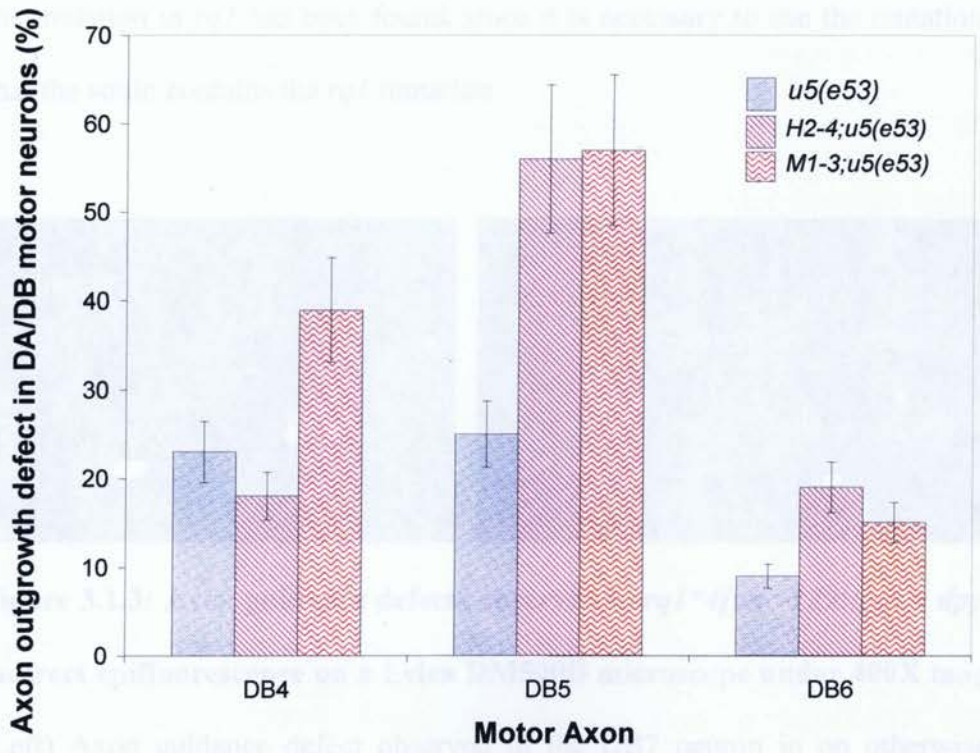

Figure 3.1.2 Axon outgrowth defects in *H2-4;unc-5(e53)* and *M1-3;unc-5(e53)*. Data shown represent the axons that failed to leave their cell bodies in the ventral cord in *unc-5(e53)* (blue bars), *H2-4;unc-5(e53)* and *M103;unc-5(e53)*. Vertical error

bars represent standard error of measurement calculated using Microsoft™ Excel® 2007 (Hatch, Lazaraton, and Dudek model). (n=60).

When the *rq1* mutation was out-crossed into the wild-type strain, axon guidance defects were observed in around 40% of animals. These defects are mild axon guidance defects and are weaker than those seen in any of the *unc-6, unc-5* or *unc-40* mutants scored to date (Figure 3.1.3). Preliminary data indicates that the *rq1;unc-40(1430)* double mutant has the same type of axon guidance defects that are seen in *unc-40* mutants suggesting that *rq1* could be in the same pathway as *unc-40*. This result needs to be confirmed once the mutation in *rq1* has been found, since it is necessary to use the mutation to confirm that the strain contains the *rq1* mutation.

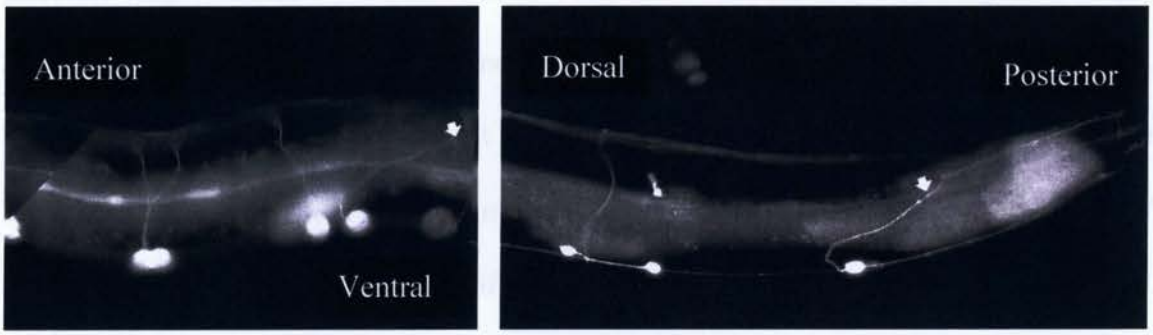

Figure 3.1.3: Axon guidance defects observed in *rq1*4[unc-129::gfp + dpy-20]* under indirect epifluorescence on a Leica DM500B microscope under 400X magnification. (Left) Axon guidance defect observed in the DB7 neuron in on otherwise wild-type background. (Right) Axon guidance defect observed in DA3 and DB4 where the two axons fuse together before reaching the dorsal cord. Around 40% of these *rq1* worms have either long-range (right) or short-range (left) or both axon guidance defects (n = 95).

Strain	DA3, DB4 fused	DB7 misguided	# of animals (n)	Percent defects (%)
N2[unc129::gfp]	0	0	107	0
*rq1*4[unc-129::gfp]*	24	13	95	40

Table 3.1.1: Axon guidance defects in *rq1[unc-129::gfp]*. *rq1* in wild-type background has both long-range (DA3, DB4 axon fusion) and short-range (DB7 misguidance) migrations of DA/DB axons. No other phenotypic defects were observed in this strain.

3.2 Microinjection of Fosmids/Cosmids

The *rq1* mutation was mapped to an interval on chromosome III by snip-SNP mapping (Sybingco, 2008). In order to identify the gene altered in the *rq1* mutant strain, genomic fragments carried on fosmids and cosmids available from the Sanger Centre or from the Moerman laboratory in Vancouver were obtained (Bueno de Mesquita, 2008). The interval contains 88 genes and it was covered by eight overlapping constructs. The eight constructs were microinjected into *rq1*3;unc-5(e53);him-5[unc-129::gfp +dpy-20]* to effect rescue of the enhancement of the axon guidance defects of *unc-5* caused by *rq1*. Microinjection experiments were conducted at Mount Sinai Hospital. Each time an injection was performed, *myo-2::yfp* expression was used as a co-injection marker (Okkema and Krause, 2005) allowing the selection of transgenic animals. This transgene emits yellow fluorescence from the pharynx of transgenic animals. In the *rq1*3;unc-5(e53);him-5* strain, the number of transgenic animals that were observed in the progeny were low because of the low brood size in this strain. Among the 9 fosmids/cosmids that were injected, only one, fosmid, H04D03, showed rescue of axon outgrowth defect phenotype of the *rq1*3;unc-5(e53);him-5* strain. The initial experiments were done by a

former graduate student and an undergraduate (Bueno de Mesquita, 2008; Kholkina, 2008). However, the number of rescued animals obtained was small, so more microinjections were performed to confirm that H04D03 is indeed the rescuing fosmid. The combined data is presented in Table 3.2.1

Fosmid/Cosmid/PCR fragment injected into *rq1;unc-5(e53)[unc-129::gfp + dpy-20]*	**# of rescued animals**	**N**	**% rescued**
H04D03	19*+17	24*+17	87
K10G9	0	0**	0
T07A5	0	15	0
T07C4	0	8	0
C38H2	0	14	0
D2045	0	8	0
F43D9	0	0**	0
T21C12	0	11	0

Table 3.2.1: Rescue data for constructs carrying DNA in the region where *rq1* was mapped. H04D03 was the only fosmid that showed rescue of axon outgrowth defects of *rq1*3;unc-5(e53);him-5[unc-129::gfp].* Rescue in this strain is not expected to be 100% because microinjected DNA can be lost from cells unless the transgene is integrated in the genome (Mello, 1991).

Note that K10G9 and F43D9 constructs were injected but no transgenic animals were obtained, possibly due to toxicity of the construct.

*Bueno-de Mesquita, M.Sc Thesis, Ryerson 2008.

Constructs contain wild-type copies of the genomic DNA from *C. elegans* and are arranged on the genome (chromosome or linkage group (LG) III as shown in Figure 3.2.1.

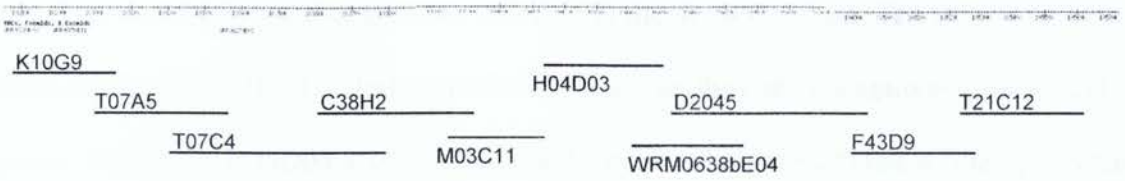

Figure 3.2.1: Fosmids/cosmids shown here which contain wildtype copy of genes in the genomic region where *rq1* was mapped to. (Image obtained from wormbase.org)

There are 6 genes that have been shown to lie within the DNA carried on the H04D03 fosmid (WormBase), so the next step was to microinject the individual genes into the double mutant. The six genes on the genomic portion of the worm genome present in H04D03 are M03C11.8, H04D03.1, H04D03.2, H04D03.3, H04D03.4, and H04D03.5. Primers were designed for each of the genes except for the last gene which was a predicted sno-RNA gene (Serdetchnaia, 2009). Each set of primers was designed so that at least 3 kb of sequence was present upstream of the gene and at least 1 kb of the 3' untranslated region was present along with the entire coding region. Each PCR reaction was made from the fosmid H04D03 and was microinjected into *rq1*3;unc-5(e53);him-5[unc-129::gfp + dpy-20]* to rescue the axon outgrowth defects. After microinjection with PCR fragments containing one of the first three genes, it was established that H04D03.1 eliminates the enhancement of axon outgrowth defects in the double mutant strain *rq1*3;unc-5(e53);him-5[unc-129::gfp + dpy-20]* (Table 3.2.2). Axon outgrowth defects in double mutants of *rq1*3;unc-5(e53);him-5[unc-129::gfp + dpy-20]* were scored as rescued when axons in three particular neurons were seen leaving the ventral nerve cord in a transgenic animal. These neurons were DB4, DB5, and DB6, which were chosen as they were easily visible against the background gut fluorescence of the animal

and these are the axons that are most affected in the double mutant. The other two genes, H04D03.2 and H04D03.3, failed to elicit rescue, so they were eliminated as candidate genes. Therefore H04D03.1 is the best candidate for the gene altered in the *rq1* mutant strain. This data implicates H04D03.1 as the rescuing gene in the *rq1*3;unc-5(e53);him-5[unc-129::gfp + dpy-20]* strain and the gene appears to have a role to play in DA/DB motor axon outgrowth in *C. elegans*.

It has been found that *rq1* has mild axon guidance defects in the DA and DB motor neurons in an otherwise wild-type background (Figure 3.1.3). Scoring the number of rescued animals in the *rq1*3;unc-5(e53);him-5[unc-129::gfp + dpy-20]* genetic background was tedious as the number of progeny in the strain was greatly reduced relative to wild-type or *unc-5(e53)* strains because this strain has a low brood size (~40 young animals per hermaphrodite). I therefore decided to microinject into the *rq1* strain and score rescue of axon guidance defects. Therefore, recent experiments have focused on rescue of the *rq1* mutation in a the *rq1* strain with only the DA/DB neuronal marker *[unc-129::gfp]* present. Using this strain, we were able to generate enough rescue data for statistical analysis. It can be seen from Table 3.2.2 that a PCR fragment containing 3 kb upstream of H04D03.1, but not one containing 1 kb of upstream sequence, can rescue the mild axon guidance defects of *rq1* in an otherwise wild-type background. More recently, the long PCR fragment of H04D03.1 was cloned by V. Serdetchnaia and it also rescues the axon guidance defects of *rq1* in an otherwise wild-type background. In addition, we found that 2 kb of upstream sequence of the H04D03.1 gene is insufficient for rescue.

To date, we have shown that the fosmid H04D03, and the long PCR fragment of H04D03.1 can rescue enhancement of the axon outgrowth defects in *rq1*3;unc-*

the axon guidance defects of *rq1* in an otherwise wild-type background. In addition, we found that 2 kb of upstream sequence of the H04D03.1 gene is insufficient for rescue.

To date, we have shown that the fosmid H04D03, and the long PCR fragment of H04D03.1 can rescue enhancement of the axon outgrowth defects in *rq1*3;unc-5(e53);him-5[unc-129::gfp + dpy-20]*. In addition, the cloned version of the long PCR product, when injected along with *myo-2::yfp* marker, can rescue the axon guidance defects of *rq1*4[unc-129::gfp + dpy-20]* in the F1, F2 and subsequent generations, so it is likely that H04D03.1 is the gene mutated in the *rq1* strain (Table 3.2.2).

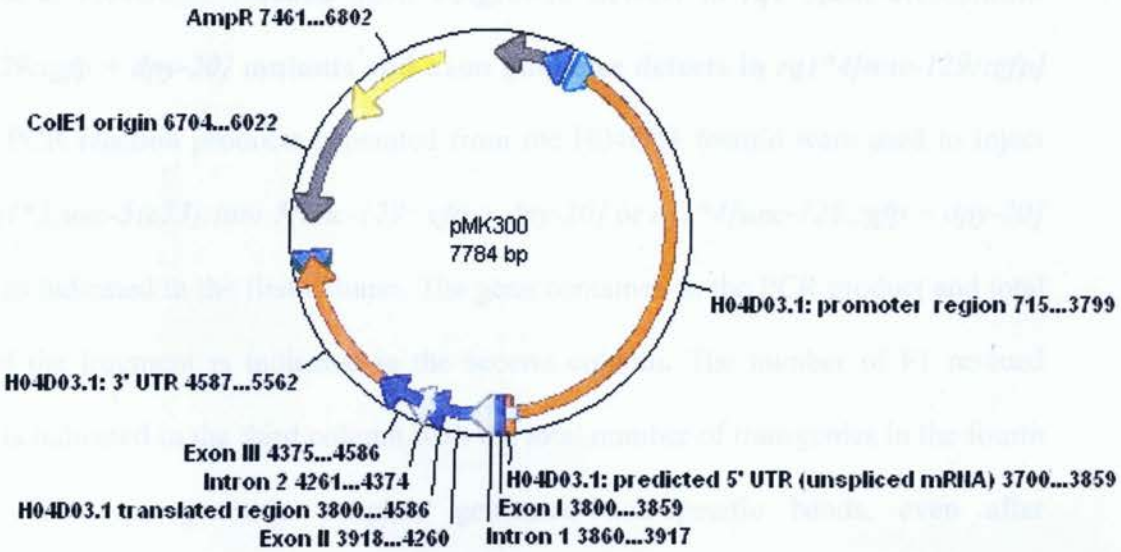

Figure 3.2.2: Cloned 4.8kb PCR fragment containing 3kb upstream of H04D03.1 and 980bp downstream. The construct also contains an Ampicillin resistant gene (AmpR).

The genomic version of the coding sequence of the H04D03.1 gene in the mutant background has been entirely sequenced and no mutation has been found to date.

Strain	PCR fragment injected	Rescued animals	N	% rescued
*rq1*3;u5(e53)[u129::gfp]*	H04D03.1 (4.8kb WT, 3kb-5', 980bp-3')	8	8	100
*rq1*3;u5(e53)[u129::gfp]*	H04D03.2 (9.1kb WT fragment)	0	7	0
*rq1*3;u5(e53)[u129::gfp]*	H04D03.3 (8.3kb WT fragment)	0	5	0
*rq1*4[u129::gfp]*	H04D03.1 (4.8kb WT, 3kb-5', 980bp-3')	47	49	96
*rq1*4[u129::gfp]*	H04D03.1 (2.8kb *rq1*, 1kb-5', 980bp-3')	0	20	0
*rq1*4[u129::gfp]*	H04D03.1 (2.8kb WT, 1kb-5', 980bp-3')	0	13	0
*rq1*4[u129::gfp]*	H04D03.1 (3.8kb WT, 2kb-5', 980bp-3')	0	11	0
*rq1*4[u129::gfp]*	pMK300 construct	12	12	100

Table 3.2.2: H04D03.1 rescued axon outgrowth defects in *rq1*3;unc-5(e53);him-5[unc-129::gfp + dpy-20]* mutants and axon guidance defects in *rq1*4[unc-129::gfp]* worms. PCR reaction products generated from the H04D03 fosmid were used to inject either *rq1*3;unc-5(e53);him-5[unc-129::gfp + dpy-20]* or *rq1*4[unc-129::gfp + dpy-20]* animals as indicated in the first column. The gene contained in the PCR product and total length of the fragment is indicated in the second column. The number of F1 rescued animals is indicated in the third column with the total number of transgenics in the fourth column. Wild-type genomic template generated non-specific bands, even after optimization of PCR reaction conditions, so the products generated from H04D03.1 were used except for line 5 where a fragment from *rq1* was used for injection (V. Serdetchnaia, personal comm.). The last line shows the data from injection of pMK300 which is a cloned version of the 4.8 kb fragment used in lines 1 and 4. The concentrations used in these injections is described in Materials and Methods but generally the co-injection marker was at 30 ng/ml.

personal comm.). The last line shows the data from injection of pMK300 which is a cloned version of the 4.8 kb fragment used in lines 1 and 4. The concentrations used in these injections is described in Materials and Methods but generally the co-injection marker was at 30 ng/ml.

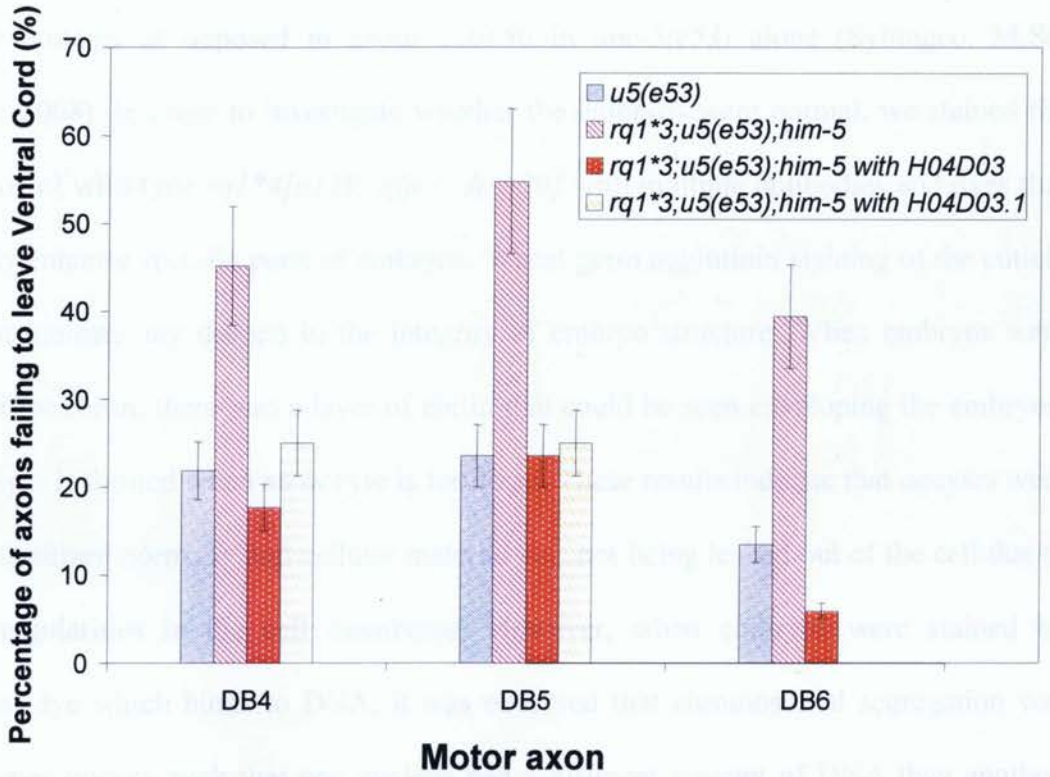

Figure 3.2.3: Graph displaying rescue data for the H04D03 fosmid and the H04D03.1 gene on PCR fragment. All strains contained *[unc-129::gfp]* for detection of the DA/DB neurons. Vertical error bars were calculated using standard error of measurement using Microsoft™ Excel® version 2007 (Hatch, Lazaraton, and Dudek model). Animals counted are listed in Table 3.2.1 and Table 3.2.2.

3.3 Embryo staining of *rq1* mutants

A separate study from the rescue experiments described above was conducted to look at apoptosis in the germ-line of the *rq1* mutant strains. In the *rq1*3;unc-5(e53);him-5[unc-129::gfp + dpy-20]* strain, the brood size was considerably lower than normal (brood size of 35±15 young animals in *rq1*3;unc-5(e53);him-5[unc-129::gfp + dpy-20]* double mutants as opposed to about 210±50 in *unc-5(e53)* alone (Sybingco, M.Sc. Thesis, 2008). In order to investigate whether the embryos were normal, we stained the embryos of wild-type *rq1*4[u129::gfp + dpy-20]* with multiple antibodies and dyes that visually enhance specific parts of embryos. Wheat germ agglutinin staining of the cuticle did not indicate any defects in the integrity of embryo structure. When embryos were stained for chitin, there was a layer of chitin that could be seen enveloping the embryos. This layer is formed when an oocyte is fertilized. These results indicate that oocytes were being fertilized normally and cellular material was not being leaked out of the cell due to any irregularities in the cell membrane. However, when embryos were stained by Hoechst dye which binds to DNA, it was observed that chromosomal segregation was sometimes uneven such that one nucleus had a different amount of DNA than another. Also, the nuclear envelope did not form properly which suggested that this defect may be causing mitotic arrest in embryos and killing them. A defect of this type could decrease the number of animals in the progeny of this strain. Since these defects are not known to occur in *unc*-5 mutants, it led us to the conclusion that the gene mutated in *rq1* could play a role in chromosomal segregation during mitosis in early embryogenesis. However, this phenotype was rare (~6%) and was not sufficient to account entirely for the reduced brood size.

causing mitotic arrest in embryos and killing them. A defect of this type could decrease the number of animals in the progeny of this strain. Since these defects are not known to occur in *unc*-5 mutants, it led us to the conclusion that the gene mutated in *rq1* could play a role in chromosomal segregation during mitosis in early embryogenesis. However, this phenotype was rare (~6%) and was not sufficient to account entirely for the reduced brood size.

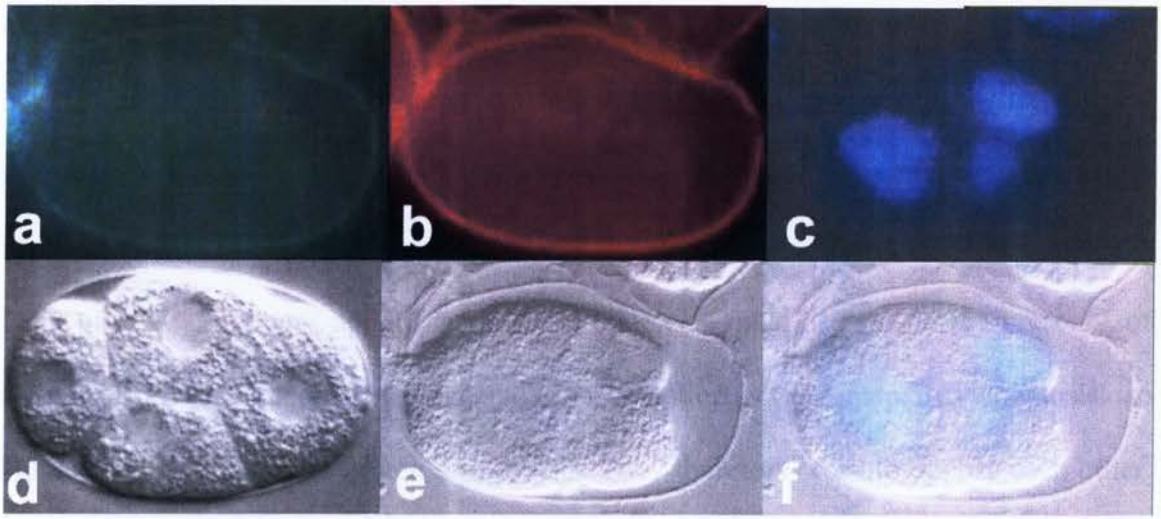

Figure 3.3.1: *rq1* embryos may have defects in cytokinesis. A) An *rq1*3;him-5[u129::gfp + dpy-20]* embryo that has been stained with wheat germ agglutinin antibody. B) Staining of chitin layer as described in Materials and Methods. C) Chromosomal DNA stained with Hoechst dye. D) DIC of the 4 cell stage of a normal *C. elegans* embryo (obtained from WormBook.org). E) DIC image of *rq1*3;him-5[unc-129::gfp]* embryo indicating abnormal cytokinesis and failure of nuclear membrane formation. F) Hoescht stained DNA image superimposed on DIC image of *rq1*3;him-5[unc-129::gfp]* embryo indicating uneven chromosomal distribution during mitotic cell division compared to that seen in d) wild type embryo (Dr. Wendy Johnston, Mt. Sinai).

worms for 3 hours as described in Materials and Methods. Strains of *rq1* in wild-type and *rq1;unc-5(e53)* were both tested in order to analyze the effects of *rq1* on germ-line apoptosis. We saw a slight increase in apoptotic cell death in *rq1[unc-129::gfp + dpy-20]* mutants which suggests that *rq1* itself might be a suppressor of apoptotic cell death (Figure 3.4.1). Surprisingly, in the *rq1;unc-5(e53)[unc-129::gfp +dpy-20]* animals, we saw that germ-line apoptosis was higher than in wild-type or *rq1* mutant animals. On the contrary, *unc-5(e53)* worms have a decrease in apoptosis relative to wild-type (Figure 3.4.1) UNC-5 has been previously described as a dependence receptor that triggers apoptosis in the developing gut (Mehlen and Bredesen, 2004). These results support the idea that both *rq1* and *unc-5* may work in two different pathways for germ-line apoptosis. Lack of UNC-5 reduces apoptosis, so some apoptosis must depend on the presence of functional UNC-5 (dependence receptor). A mutation in *rq1* increases apoptosis, so H04D03.1 must normally decrease apoptosis. They therefore work to oppose each other. However, the fact that the level of apoptosis is increased in absence of UNC-5 and a mutation in H04D03.1, indicates that the mutation in *rq1* overides the lack of UNC-5. This is an interesting possibility and should be investigated further by following apoptotic corpses over time with DIC in the developing gonad.

According to the dependence receptor hypothesis (Mazelin *et al*, 2004), the absence of UNC-6/Netrin triggers cell death but its presence supports cell survival, as long as the ligand can bind to one of its receptors, either UNC-5 or UNC-40. In the *C. elegans* germ-line the absence of UNC-6 increases apoptosis as expected if the dependence receptor hypothesis is correct, while an absence in either of the 'triggers' (the receptors) decreases apoptotic cell death in the gonad (Figure 3.4.1). Furthermore, our

observations indicate that *unc-40* has lower apoptosis in the germ-line than *unc-5*, suggesting that *unc-40* plays a more important role in regulating germ-line apoptosis than *unc-5*. This is a novel finding as this was not previously described in *C. elegans* and further work on time courses should be done in the future.

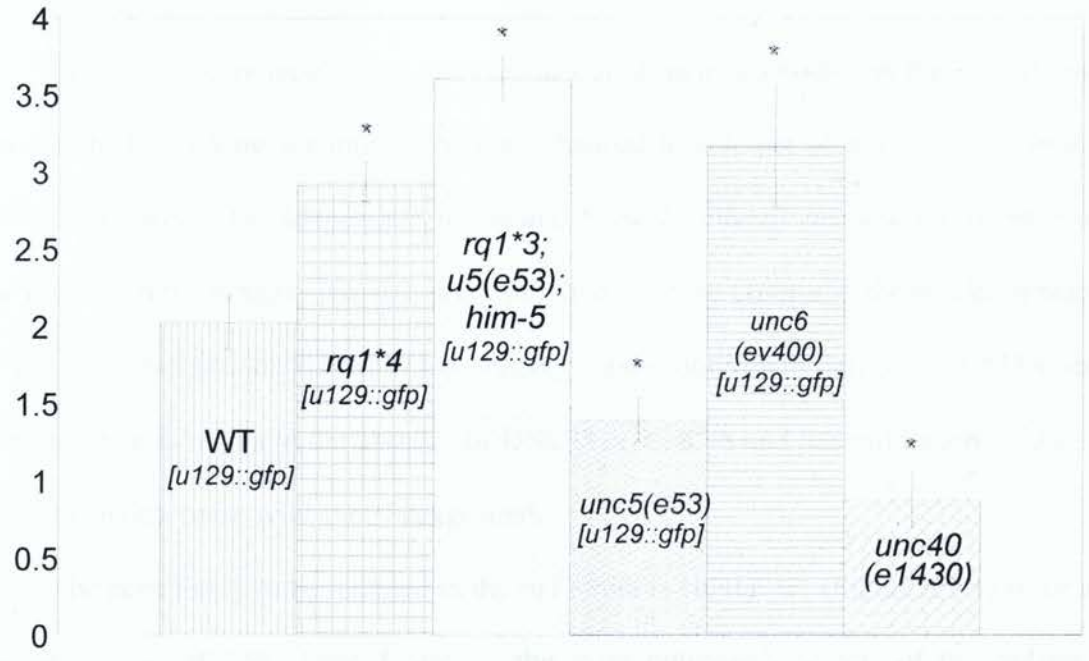

Figure 3.4.1 Germline apoptosis is increased in an *rq1;unc-5(e53)* double mutant background relative to *unc-5* background (N= 3 sets of 20). There are approximately two corpses per gonad arm in wild-type animals (vertical lines). *rq1*4* animals (grid) have a slight increase in corpses per gonad arm relative to wild-type animals. Surprisingly, *rq1*3;unc-5(e53);him-5* animals have a further increase in corpses per gonad arm (dots). *unc-5(e53)* mutants (waves) have a lower level of germ-line apoptosis than wild-type animals. This is in agreement with the dependence receptor hypothesis. Lack of UNC-6 (horizontal lines) caused elevated levels of apoptosis and lack of UNC-40 (bricks) caused decreased levels of apoptosis in accordance with the dependence receptor hypothesis.

*Difference from *WT[unc129::gfp]* is statistically significant for one-tailed t-test ($p<0.05$)

4.0 Discussion

In this study, molecules that steer axons out of their cell bodies in the ventral cord were sought by looking for mutations that enhanced this defect of *unc-5(e53)* animals. Such mutants would be independent of the *unc-5/unc-6* pathway because the screen was done in *unc-5* null animals. The *rq1* strain satisfied all these criteria as the results indicate that the gene mutated in this strain has enhanced axon outgrowth defects in the DA and DB motor neuron axons in the absence of UNC-5 or UNC-6 and has mild axon guidance defects in an otherwise wild-type background.

The gene likely to be mutated in the *rq1* strain is H04D03.1 (Figure 4.0.1) since a) injection of the H04D03 fosmid rescued the axon outgrowth defects of the *rq1;unc-5(e53)* mutant strain and several other cosmids failed to do this b) a 4.8 kb PCR fragment containing the H04D03.1 gene along with 3 kb of 5' regulatory sequence and 1 kb of 3' untranslated sequence rescued the outgrowth defects, c) a cloned version of the same 4.8 kb PCR fragment rescued the axon guidance defects of the *rq1* mutants. Furthermore, I have shown that a PCR fragment containing either 1 kb or 2 kb upstream of the H04D03.1 gene does not rescue the axon guidance defects of *rq1*, suggesting that more than 2 kb and up to 3 kb of 5' regulatory sequence is required to effect rescue of the defects.

According to homology searches, H04D03.1 is a novel protein with four other highly homologous proteins in *C. elegans* but weak similarity to proteins in other organisms. The other proteins are W03G9.3, (bit score of 313 and E value of $5e^{-84}$, LG I), C38D4.1, (bit score 310, E value of $6e^{-83}$, LG III), W05F2.2, (bit score of 298, E value of $2e^{-79}$, LG I), and Y37D8A.12, (bit score of 293, E value of $5e^{-78}$, LG III). The other four

proteins are also novel and also uncharacterized, so a new type of protein may have been uncovered by this study.

According to the Transmembrane Helix prediction algorithm (TMHMM) found on WormBase, H04D03.1 is a transmembrane protein with an amino terminal region containing a potential transmembrane domain (amino acids 6-36), followed by a predicted region outside the membrane, and a second transmembrane domain (amino acids 108-129). Since the protein is predicted to be associated with the membrane, it could mean that H04D03.1 is a receptor like UNC-5 and UNC-40 that mediates axon guidance through aid from extracellular graded ligand cues like UNC-6. However, from the discussion below, it seems more likely to be some kind of novel ion channel. Proper biochemical analysis is needed to further elucidate the true role of H04D03.1 in DA/DB motor axon guidance.

Protein sequence of H04D03.1 obtained from wormbase.org:

MRILRILFSLVIFGLIVHVLPTTTTPNVPVSAATNTSNVTAPAGNSTKSPNATAPAG
NSTKNVNVTALSANTTQLALVSSASPETCKNGNGTHCPSRTISFHKDTPKYIGCGI
LIAFVIFHIFLYFYLEDQKAREQKKYFEELIAEQMAARKREEQDEKQHEDEEMLC
RLRIGVSKDRKREEQDDQQHEDEAPEAVVTVDKPRD

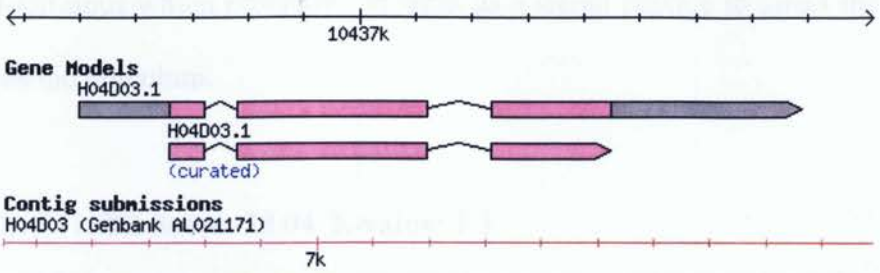

Figure 4.0.1: H04D03 conceptual map showing three predicted exons in the open reading frame of the gene. No other splice variations are predicted for this gene (wormbase.org).

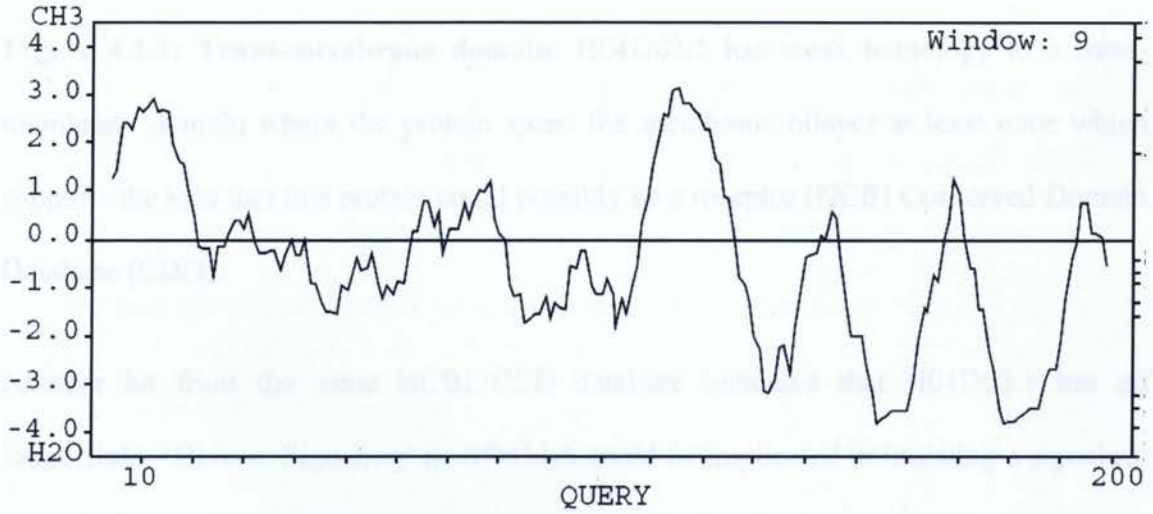

Figure 4.0.2: Hydropathy plot for H04D03.1. The plot indicates two highly hydrophobic motifs in the protein which suggests that this protein could be spanning the membrane region (Kyte and Doolittle method).

4.1 Domain homology of H04D03.1 with non-*C. elegans* proteins:

Since H04D03.1 is a novel protein, its biochemical function in the nematode can only be speculated upon by looking at its conserved domains and interacting motifs. According to several homology searches, this protein has an integral membrane domain

near the N-terminus which probably functions as a signal peptide to direct the protein to the endoplasmic reticulum.

CD Length: 141 **Bit Score:** 28.04 **E-value:** 1.3

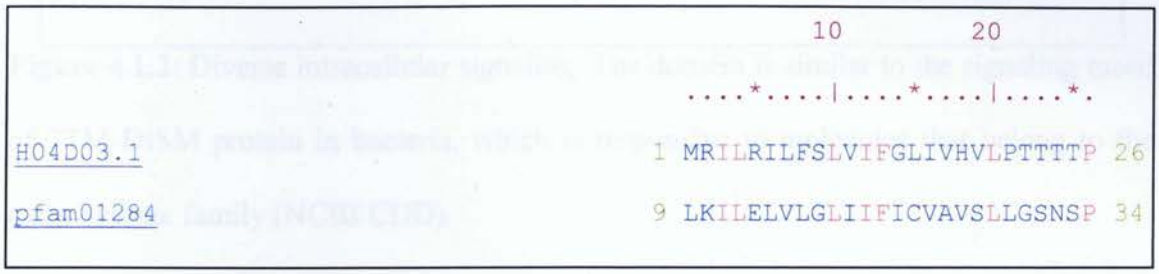

Figure 4.1.1: Trans-membrane domain. H04D03.1 has weak homology to a trans-membrane domain where the protein spans the membrane bilayer at least once which supports the idea that this protein could possibly be a receptor (NCBI Conserved Domain Database (CDD).

Another hit from the same NCBI CCD database indicated that H04D03.1 has an intracellular 'Diverse Signaling' motif which could be implicated in initiating a signaling cascade that would direct the growth-cone of an actively migrating axon. The protein that this part is homologous to is called 7TM-DISM, which is a trans-membrane molecule found in bacterial cells. This protein seems to respond to extracellular cues that belong to the carbohydrate family of molecules (Aravind *et al*, 2003).

CD Length: 206 **Bit Score:** 30.72 **E-value:** 0.19

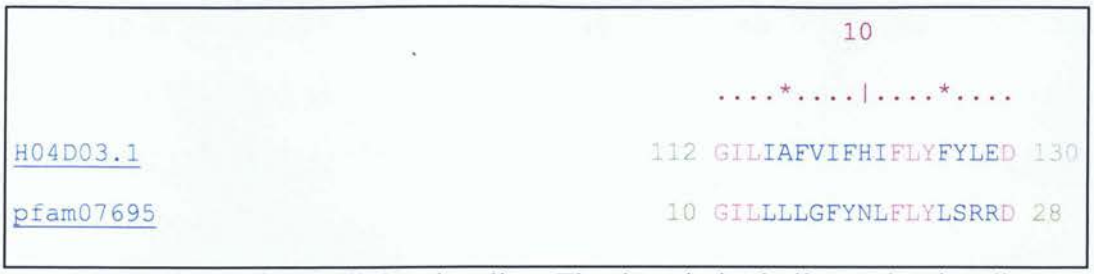

Figure 4.1.2: Diverse intracellular signaling. The domain is similar to the signaling motif of 7TM-DISM protein in bacteria, which is responsive to molecules that belong to the carbohydrate family (NCBI CDD).

H04D03.1 also has some homology with a Na+/H+ antiporter subunit (an E-value of 0.066) which suggests that this protein could be involved in maintaining pH inside the cell and also keep Na+ homeostasis in check. These two activities are closely related to neurons because after an action potential is completed in an axon, they are filled with positive ions such as Na+ and it is with the help of proteins like Na+/H+ antiporters that are able to regain their pre-action potential state (Padan and Schuldiner, 1993).

Antiporter systems do not necessarily play a role in axon guidance however, they are crucial for maintaining integrity of an axon. If H04D03.1 is an antiporter system, a mutation in this protein could degenerate neurons which rely on it for homeostasis. According to the data shown in Figure 3.1.1, we see that not all motor neurons axons are affected by *rq1* mutation which could imply that either the gene is under-expressed, the mutation is a hypomorph, or this protein is redundant in axon guidance pathway.

CD Length: 197 **Bit Score:** 32.39 **E-value:** 0.066

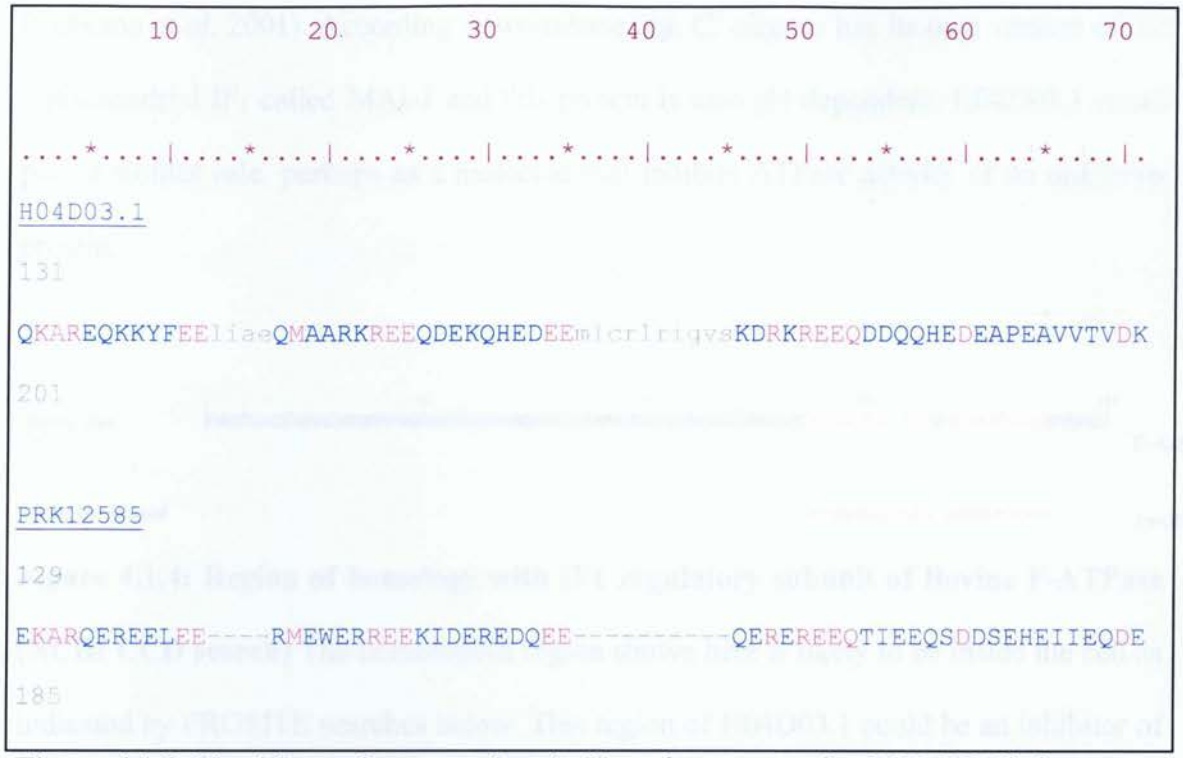

Figure 4.1.3: Na+/H+ antiportor subunit. Homologous protein PRK12585 belongs to a cation/proton antiporter family which has orthologs in several species such as in *Rhizobium meliloti* (PhaG), *Staphylococcus aureus* (MnhG), and *Bacillus subtilis* (YufB). Red indicates homologous residues (Padan and Schuldiner, 1993).

In a similar context, NCBI closely related protein database indicated that H04D03.1 is most similar to a regulatory subunit of a mitochondrial ATPase known as IF_1 in the species *Bos Taurus* (Fig. 4.1.4). The protein is a subunit of the ATP sythase but only the ATPase activity is inhibited by the minimal inhibitory region of the protein IF_1 (Raaig *et al*, 1996) and not the ATP synthase. The minimal ATPase inhibitory region is found within the region of homology shown below. This regulatory subunit is pH dependent, dimerizing at low pH and binding stably to the ATPase complex to inhibit it. At high pH,

IF_1 is an inactive tetramer, which activates the ATPase complex in mitochondria (Cabezon *et al*, 2001). According to wormbase.org, *C. elegans* has its own version of the mitochondrial IF_1 called MAI-1 and this protein is also pH dependent. H04D03.1 could play a similar role, perhaps as a molecule that inhibits ATPase activity of an unknown protein.

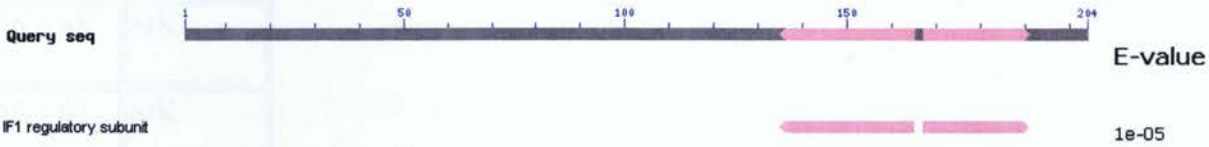

Figure 4.1.4: Region of homology with IF1 regulatory subunit of Bovine F-ATPase (NCBI CCD search) The homologous region shown here is likely to be inside the cell as indicated by PROSITE searches below. This region of H04D03.1 could be an inhibitor of ATPase activity of a yet unknown protein that could be involved in axon migration.

According to several PROSITE searches, the N-terminus of H04D03.1 contains 8 potential glycosylation sites (Table 4.1.1). Since glycosylation sites are normally found on the exposed surface of membrane proteins, it is possible that the N-terminus and all 8 glycosylation sites are located extracellularly or in the lumen of organelles.

35-38	58-61	64-67	38-41	45-48	51-54	71-74	90-93
NTSN	NSTK	NVTA	NVTA	NSTK	NATA	NTTQ	NGTH

Table 4.1.1: N-glycosylation sites on H04D03.1. These motifs are close to the N-terminus of the protein which indicates that the N-terminus of H04D03.1 is possibly on the surface of the neuronal cell membrane.

Further homology hits indicate that this protein also has several potential Protein kinase C phosphorylation sites (Table 4.1.2). If these sites are exposed at the surface of the protein at a specific point in time, it is possible that the protein has an active and an inactive form based upon its phosphorylation state.

46 – 48	StK
59 – 61	StK
85 – 87	TcK
105 - 107	TpK

Table 4.1.2: Protein kinase C phosphorylation site on H04D03.1 suggests that this protein could be phosphorylated to become active and perform its function.

From residues 112-117 (GIliAF) is a putative N-myristoylation site. Attachment sites for myristate, a C14-saturated fatty acid. N-myristoylation tes have several requirements that allows them to be distinctive and only be present in a handful of proteins. These requirements are as follows:

- N-terminal residue at this site must be a glycine residue where myristate binds
- Only uncharged residues are allowed in position 2 but proline and large hydrophobic residues are not allowed
- All residues are allowed in positions 3 and 4
- Position 5 must contain only small uncharged amino acids
- All amino acids are allowed at position 6 except for proline

4.2 H04D03.1 interacts with ZEN-4 and GEI-4

Yeast-two-hybrid (Y2H) screens indicate that H04D03.1 interacts with a well characterized *C. elegans* protein called ZEN-4/MKLP1 (ZEN is for Zygotic ENclosure defective) and a recently discovered intermediate filament regulatory protein called GEI-4 (GEI is for GEx Interacting) (Li *et al*, 2004). These particular interactions could very well explain the embryonic lethality defects that were observed in *rq1* strains during antibody and Hoescht staining of *rq1* embryos.

GEI-4 is a protein that is implicated in the cytoskeletal rearrangement during embryo development and is an essential regulatory unit of a larger complex containing two other proteins namely GEX-2 and GEX-3. The protein is not well characterized itself but it is known through antibody staining that it localizes at the site of GEX-2/GEX-3 proteins and also that when *gei-4* expression was reduced using RNAi, embryos became non-viable with visible tissue defects. This indicates that the protein is essential for embryo development and morphogenesis (Tsuboi *et al*, personal communication). Since embryonic defects were seen in *rq1* strains, absence of H04D03.1 could affect normal function of the GEI-4 protein.

The ZEN-4 protein is involved in segregation of chromosomes during the metaphase period of cell division inside a *C. elegans* embryo (Raich *et al,* 1998). Since chromosomal segregation greatly depends on formation of several microtubular elements (Sawai, 1992), ZEN-4 is believed to have a role to play in microtubule development and regression (Raich *et al,* 1998). This protein has 28-31% homology to the CHO1/MKLP1 class of motor proteins which accumulate at the mid-zone of the microtubulular spindle during metaphase and are crucial for ensuring proper microtubule attachment and

segregation of chromosomes during metaphase (Hirokawa, 1998). After the metaphase event however, proteins belonging to the CHO1/MKLP1 family do not have an essential part to play as it was observed that antibodies targeting these proteins, when injected in embryos after metaphase, did not hinder normal development of internal cell mass and daughter nuclei formation (Nislow *et al*, 1990). Since ZEN-4 is homologous to members of the CHO1/MKLP1 family of proteins, it was initially assumed that ZEN-4 would be associated with mid-zone microtubule assembly (Raich *et al*, 1998). This idea was verified using antibodies against ZEN-4 during metaphase of cell division. In *zen-4* null animals, the central spindle was not seen during metaphase but was observed in wild-type animals as shown in Figure 4.2.1 (Raich *et al*, 1998).

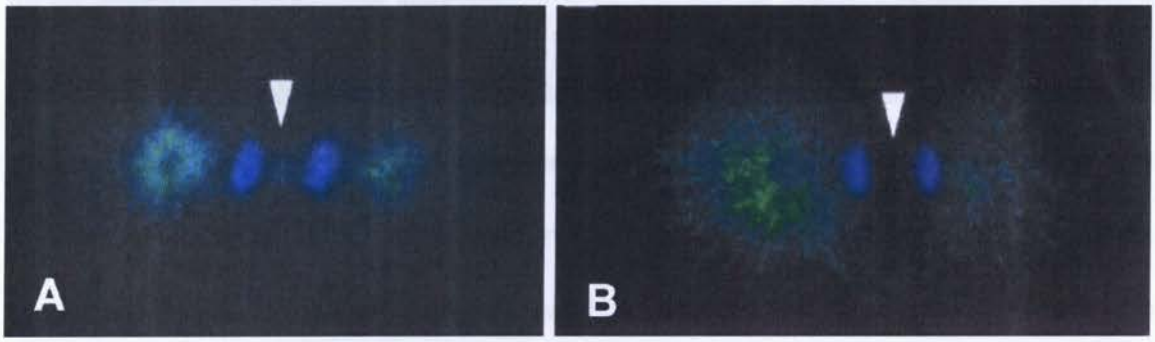

Figure 4.2.1: Metaphase of a cell in *C. elegans* embryo. A) Single cell mass in wild-type embryo undergoing cell division; arrow pointing at central spindle formation. B) *zen-4* null animals do not show central spindle formation. Green is β-tubulin antibody and blue indicates DAPI staining of DNA (Raich *et al*, 1998).

Aside from helping central spindle formation and unlike the CHO1/MKLP1 proteins, ZEN-4 is also required for cytokinesis where it helps in formation of the cleavage furrow (Raich *et al*, 1998). This characteristic was observed when *zen-4* null mutants exhibited

defects in cytokinesis during experiments determining the spatial and temporal localization of ZEN-4 protein (Raich *et al*, 1998). The observation was verified using two methods; first, to look at embryos of animals with no ZEN-4 expression in their germ-line and second, looking at embryos of animals which were injected with dsRNA to suppress *zen-4* mRNA translation. In both types of animals, cells dividing inside an embryo were not able to undergo cytokinesis and were left with multinucleated cell masses which lead to the conclusion that ZEN-4 is essential for both central spindle assembly as well as cytokinesis (Raich *et al*, 1998).

Figure 4.2.2: Cytokinesis in *C. elegans* embryo. A) Cells in wild-type embryo (*) undergoing mitotic cell division with two daughter nuclei (x) and cell membrane formation. B) RNAi for *zen-4*; no cell membrane is seen and three daughter nuclei are present in the cell mass. C) Embryo of a *zen-4* null animal showing minimal cleavage furrow and no cell membrane to separate the multiple daughter nuclei (Raich *et al*, 1998).

This defect is similar to what is seen in a few *rq1* embryos (less than 5%) which could suggest that H04D03.1 interaction with ZEN-4 is required for normal embryo development. However, absence of this defect in most *rq1* embryos could also suggest that either the H04D03.1 allele that is present in *rq1* is a hypomorph or, ZEN-4 has other partners that could replace H04D03.1 during cell division.

4.3 *unc-5* and *unc-40* behave like dependent receptors for *unc-6*

As previously mentioned, mammalian homologues of *unc-5* and *unc-40* seem to trigger apoptosis in basal stem cells of the gut in the absence of *unc-6* signalling. This seems to be the case in *C. elegans* germ-line as well. According to the results that are presented in Figure 3.4.1, absence of *unc-6* signalling increases germ-line apoptosis while absence of either *unc-5* or *unc-40* decreases the number of dead cells found inside the gonad. These genes are essential factors in axon guidance and do not trigger apoptosis in the nerve cells in the absence of UNC-6. However, they seem to respond differently when working in the germ-line. In the case of both the mammalian and nematode models, it can be seen that these two receptors are dependent on UNC-6 signalling for inhibiting or triggering apoptosis.

In the case of *rq1* strains, the H04D03.1 gene seems to works as an anti-apoptotic gene because in the absence of the putative protein, germ-line apoptosis increases. Even though the increase is small, around 1.0 ± 0.2 cells higher than *WT[u129::gfp]*, it is none the less significant ($p<0.05$). In *rq1* and *unc-5* double mutants however, germ-line apoptosis increases dramatically, around 1.6 ± 0.2 cells higher than *WT[u129::gfp]*, which suggests that H04D03.1 and UNC-5 are working in separate pathways even in germ-line apoptosis. Nothing more could be said about the role of H04D03.1 in apoptosis and its interactions with other receptor proteins until further biochemical analyses are performed.

Rescue of this defect could not be performed because apoptosis analysis requires a large data set containing 60 animals and there has been no progress in producing this many transgenic animals using plasmid microinjections.

5.0 Future work

To confirm that H04D03.1 is involved in axon guidance of DA/DB motor neurons, additional evidence needs to be provided besides those reported in this study, which was injecting wild-type copies of genes to rescue the mutant phenotype. Most importantly, a H04D03.1 gene knockout mutant has to be made to see if the DA/DB axon guidance defects are present in that null animal. Finding a mutation in the remaining sequence of the H04D03.1 gene would be good evidence that this is the gene mutated in the *rq1* strain. The temporal and spatial expression patterns of this gene should also give important clues about the potential roles of this protein in axon guidance. If it is expressed in the neurons it may function cell autonomously for axon guidance. If it is expressed instead outside the neurons it must play a cell non-autonomous role and may function to guide the axon around the body of the worm. Temporal expression patterns could be generated by placing a fluorescent protein gene under the control of the H04D03.1 promoter. As for localization of H04D03.1 protein, a tagged version of this protein should be made where either the tag is fluorescent and indicates the localization of the protein or, the tag is a binding site for antibodies which could carry a fluorescent tag with them.

In the case of germ-line apoptosis and cell division, it will be necessary to see if the apoptotic defects in the *rq1* mutant are rescued by wild-type copies of the H04D03.1 gene. Biochemical analysis should to be done to see if the H04D03.1 protein elutes with known apoptotic triggers and proteins which are involved in cellular division in *C. elegans* embryo. Further analyses including time course analysis of apoptosis in animals subjected to mutagens need to be examined. Exposure to mutagens may elevate levels of

apoptosis and could provide further support to the existing data since exposure to mutagens will increase the levels of apoptosis and may accentuate the effects of the mutations on the appearance of the numbers of apoptotic corpses in the various mutant strains.

6.0 Conclusion

A starting hypothesis in this work was that the gene altered in the *rq1* mutant could be rescued by wild-type copies of DNA in the region of the genome where the mutation had been previously mapped by snip-SNP analysis (Sybingco 2008). It was known that the fosmid H04D03.1 rescued the mutant defects (Bueno de Mesquita, 2008). In this study, rescue of the mutant motor axon outgrowth defects in *rq1;unc-5(e53)* and axon guidance defects of *rq1* in an otherwise wild-type background by microinjected genes from H04D03 were scored and they were both rescued by a single gene called H04D03.1. From our genetic enhancer screen for axon guidance defects of the DA/DB motor neurons in an *unc-5(e53)* mutant background, we suggest that H04D03.1 may be involved in axon migration of these neurons. The gene is likely to be acting in a pathway parallel to the *unc-5/unc-6* pathway. This gene also seems to play a role in cell division during embryogenesis where it could be working with proteins such as ZEN-4 for aiding in microtubule formation, chromosomal segregation, and cytokinesis. Furthermore, H04D03.1 is also implicated as an anti-apoptotic gene as in its absence, a higher number of apoptotic events takes place in the germline. This supports the hypothesis that genes involved in nervous system formation could affect apoptosis. Once the nature of the mutation in the *rq1* strain is known, it will be easier to establish the importance of the protein in these activities. If the protein is under-expressed or the mutation suggests a hypomorph it is possible that a null mutation may be lethal since the gene may encode an essential protein. Knock-out strains have been requested from three groups with specialization in *C. elegans* knock-out methodology. Once these are available, the necessity for the H04D03.1 protein in axon guidance of other neurons and its

involvement in germ-line apoptosis can be investigated more fully. This current study provides tantalizing evidence for the existence of a novel protein pathway that may be involved in axon guidance of motor neurons.

7.0 References:

Ackley, B.D., Crew, J.R., Elamaa, H., Pihlajaniemi, T., Kuo, C.J., Kramer, J.M. 2001. The NC1/Endostatin Domain of *C. elegans* type XVIII collagen affects cell migration and axon guidance. Journal of Cell Biology. **152**, 1219-1232

Aravind, L., Anantharaman, V. 2003. Application of comparative genomics in the identification and analysis of novel families of membrane-associated receptors in bacteria. BMC Genomics. **4**, 34

Brenner, S. 1974. The genetics of *Caenorhabditis elegans*. Genetics. **77**, 71-74

Bueno de-Mesquita, M. 2008. Characterization of *rq1*, a mutant involved in nervous sytem development in *C. elegans*. M.Sc Thesis, Ryerson University.

Cabezon, E., Arechaga, I., Jonathan, P., Butler, G., Walker, J.E. 2001. Dimerization of the F1-ATPase by binding the inhibitor protein, IF1. Journal of Biological Chemistry. **275**, 28353-28355

Chan, S.S. Y., Zheng, M.W., Wilk, R., Killeen, M.T. 1996. UNC-40, a *C. elegans* homologue of DCC (Deleted in Colorectal Cancer), is required in motile cells responding to UNC-6 netrin cues. Cell. **87,** 187-195

Colavita, A., and Culotti, J.G. 1998. Supressors of ectopic UNC-5 growth cone steering identify eight genes involved in axon guidance in *Caenorhabditis elegans*. Dev. Biol. **194**, 72-85

Colavita, A., Krishna, S., Zheng, H., Padgett, R.W., Culotti, J.G. 1998. Pioneer Axon Guidance by UNC-129, a *C. elegans* TGF-B. Science. **281**, 706-709

Davis, M. W., Hammarlund, M., Harrach, T., Hullett, P., Olsen, S., and Jorgensen, E. M. 2005. Rapid single nucleotide polymorphism mapping in *C. elegans*. BMC Genomics. **6**, 118.

Derry, W.B., Putzke, A.P., Rothman, J.H. 2001. *Caenorhabditis elegans* p53: Role in Apoptosis, Meiosis, and Stress Resistance. Science. **294**, 591-595

Dodd, J. and Jessell, T.M. 1988. Axon guidance and the patterning of neuronal projections in vertebrates. Science. **242**, 692-699

Gao, M.X., Liao, E.H., Yu, B., Wang, Y., Zhen, M., Derry, W.B. 2008. The SCF^{FSN-1} ubiquitin ligase controls germline apoptosis through CEP-1/p53 in *C. elegans*. Cell Death and Differentiation. **15**, 1054-1062

Gumienny, T.L., Lambie, E., Hartwieg, E., Horvitz, H.R., Hengartner, M.O. 1999. Genetic control of programmed cell death in *Caenorhabditic elegans* hermaphrodite germline. Development. **126**, 1011-1022

Hao, J., Fujisawa, K., Culotti, J.G., Gengyo-Ando, K., Mitani, S., Moulder, G., Barstead, R., Tessier-Lavigne, M., Bargmann, C. 2001. *C. elegans* Slit Acts in Midline, Dorsal-Ventral, and Anterior-Posterior Guidance via the SAX-3/Robo Receptor. Neuron. **32**, 25-38

Hedgecock, E.M., Culotti, J.G., Hall, D.H. 1990. The *unc-5*, *unc-6*, and *unc-40* genes guide circumferential migration of pioneer axons and mesodermal cells on the epidermis in *C. elegans*. Neuron. **4**, 61-85

Hengartner, M.O., Lettre, G. 2006. Developmental apoptosis in *C. elegans*: a complex CEDnario. Nature Reviews Molecular Cell Biology. **7**, 97-108

Hirokawa, N. 1998. Kinesin and dynein superfamily proteins and the mechanism of organelle transport. Science. **279**, 519-526

Hope, I.A. 1999. *C. elegans*: A practical approach. P.A.S. NewYork, Oxford University Press.

Ishi, N., Wadsworth, W.G., Stern, B.D., Culotti, J.G., Hedgecock, E. 1992. Unc-6, a laminin-related protein, guides cell and pioneer axon migrations in *C. elegans*. Neuron **9**, 873-881

Jin M, Guan CB, Jiang YA, Chen G, Zhao CT, Cui K, Song YQ, Wu CP, Poo MM, Yuan XB. 2005. Ca2+-dependent regulation of Rho GTPases triggers turning of nerve growth cones. Journal of Neuroscience. **25**, 2338-2347.

Johnson GL, Lapadat R. 2002. Mitogen-activated protein kinase pathways mediated by ERK, JNK, and p38 protein kinases. Science. **298**, 1911–1912

Johnston, W.L., Krizus, A., Dennis, J.W. 2006. The eggshell is required for meiotic fidelity, polar-body extrusion and polarization of the *C. elegans* embryo. BMC Biology. **4**, 35

Keleman, K. and Dickson, B.J. 2001. Short- and long-range repulsion by the *Drosophila* Unc5 netrin receptor. Neuron. **32**, 605-617

Killeen, M. T., Tong, J., Krizus, A., Steven, R., Scott, I., Pawson, T., Culotti, J. 2002. UNC-5 function requires phosphorylation of cytoplasmic tyrosine 482, but its UNC-40-independent functions also require a region between the ZU-5 and death domains. Developmental Biology, **251**, 348-366.

Kholkina, G. 2008. Microinjection of cosmid DNA to rescue *C. elegans* mutants exhibiting axon guidance defects. Undergraduate thesis Ryerson University.

Lee J, Li W, Guan KL. 2005. SRC-1 mediates UNC-5 signaling in *Caenorhabditis elegans*. Molecular Cell Biology. **25,** 6485-6495.

Leung-Hagesteijn, C., Spence, A.M., Stern, B.D., Zhou, M. W. 1992. UNC-5, a transmembrane protein with immunoglobulin and thrombospondin type 1 domains, guides cell and pioneer axon migrations in *C. elegans*. Cell. **71**, 289-299

Li S *et al.* 2004. A map of interactome network of the metazoan *C. elegans*. **303**. 540-543

Lin, Z. and Floros, J. 2000. Rapid Mini-Scale plasmid isolation for DNA sequencing and Restriction Mapping. BioTechniques. **29**, 466-468

MacNeil, L.T., Hardy, W.R, Pawson, T., Wrana, J.L., Culloti, J.G. 2009. UNC-129 regulated the balance between UNC-40 dependent and independent UNC-5 signaling pathways. Nature Neuroscience. **12**, 150-155

Mazelin, L., Brenet, A., Bonod-Bidaud, C., Pays, L., Arnaud, S., Gespach, C., Bredesen, D., Scoazec, J., Mehlen, P. 2004. Netrin-1 controls colorectal tumorigenesis by regulating apoptosis. Nature. **431**, 80-84

Mehlen, P., Bredesen, D.E. 2004. The dependence receptor hypothesis. Apoptosis. **9**, 37-49

Mello, C. C., Kramer, J. M., Stinchcomb, D., Ambros, V. 1991. Efficient gene transfer in *C. elegans*: extrachromosomal maintenance and integration of transforming sequences. EMBO. **10**, 3959-3970.

Merz, D.C., Zheng, H., Killeen, M.T., Krizus, A., Culotti, J.G. 2001. Multiple signaling mechanisms of the UNC-6/netrin receptors UNC-5 and UNC-40/DCC *in vivo*. Genetics. **158**, 1071-1080

Miller, D.M., Stockdale, F.E., Karn, J. 1986. Immunological identification of the genes encoding the four myosin heavy chain isoforms of *C. elegans*. PNAS. **83**, 2305-2309

Nislow, C., Sellitto, C., Kuriyama, R., McIntosh, J.R. 1990. A monoclonal antibody to a mitotic microtubule-associated protein blocks mitotic progression. Journal of Cell Biology. **111**, 511-522

Okkema, P.G., Krause, M. 2005. Transcriptional regulation. WormBook. **23**, 1-40.

Padan, E., Schuldiner, P., Taglicht, D., Rimon, A., Olami, Y., Gerchman, Y. 1993. Histidine-226 is part of the pH sensor of NhaA, a Na+/H+ antiportor in *Escherichia coli*. PNAS. **4**, 1212-1216

Raich, W.B., Moran, A.N., Rothman, J.H., Hardin, J. 1998. Cytokinesis and Midzone Microtubule organization in *C. elegans* require the kinesin-like protein ZEN-4. Molecular Biology of the Cell. **9**, 2037-2049

Round, J. and Stein, E. 2007. Netrin signaling leading to directed growth cone steering. Current Opinion in Neuronbiology. **17**, 15-21

Sawai, T. 1992. Effect of microtubular poisons on cleavage furrow formation and induction of furrow-like dent in amphibian eggs. Development and Growth Differenciation. **34**, 669-675

Serafini, T., Kennedy, T.E., Galko, M.J., Mirzavan, C., Jessell, T.M., Tessier-Lavigne, M. 1996. The netrins define a family of axon outgrowth-promoting proteins homologous to C. Elegans UNC-6. Cell. **79**, 409-424

Serdetchnaia, V. 2009. Research towards identification of the gene altered in the *rq1* axon guidance mutant of *C. elegans*. Undergraduate thesis Ryerson University

Sybingco, S. 2008. Identification and analysis of novel mutants exhibiting defects in pioneer axon guidance in *C. elegans*. M.Sc Thesis, York University.

Tong J, Killeen M, Steven R, Binns KL, Culotti J, Pawson T. 2001. Netrin stimulates tyrosine phosphorylation of the UNC-5 family of netrin receptors and induces Shp2 binding to the RCM cytodomain. Journal of Biological Chemistry. **276**, 40917-40925

Wadsworth, W.G. 2002. Moving around in a worm: netrin UNC-6 and circumferential axon guidance in *C. elegans*. Trends in Neurosciences. **25**, 423-429

Wadsworth, W.G., Bhatt, H., Hedgecock, E.M., 1996. Neuroglia and pioneer neurons express UNC-6 to provide global and local Netrin cues for guiding migrations in *C. elegans*. Neuron. **16**, 35-46.

White, J., Southgate, E., Thomson, J., Brenner, S. 1976. The structure of the Ventral nerve cord of *Caenorhabditis elegans*. Philosophical Transactions of the Royal Society of London. Series B. Biological Sciences. **275**, 327-348

Zallen, J.A., Kirch, S.A., Bargmann, C.I. 1999. Genes required for axon pathfinding and extension in the *C. elegans* nerve ring. Development. **126**, 3679-3692

8.0 Appendix

Primers used to sequence H04D03.1 on H04D03 fosmid

H04D03.1 Forward	AAGCGAATTGCGTACTCCACG
H04D03.1 Reverse	GAATTGCCGGCAGGAGCGGTC

Primers used to amplify H04D03.1 gene for microinjection

H04D03.1 Forward (for 4.8kb fragment, 3kb-5')	GTACTGCAGCGTTGATTCGAGCCTGTTGAAGGAG
H04D03.1 Reverse (for 4.8kb fragment, 980bp-3')	GTGCTGCGGCCGCTCTTAACCATGCAAAATCAG
H04D03.1Forward (1kb upstream of start codon)	ACTGCGGCCGCACGTACCACCGTATTTGATTCC
H04D03.1Reverse (700kb downstream of stop codon)	ATTCTGCAGTTCGATTAGCCCGCCACCGTG
H04D03.1Forward (2kb upstream of start codon)	ATCGCGGCCGCGAGCAAAATCGTTCGAATATTG
H04D03.2 Forward (for 9.1kb WT fragment)	GCTAGCGGCCGCATAGACCACATCACTACAG
H04D03.2 Reverse (for 9.1 kb WT fragment)	CGTACTGCAGCCAACAACCACCACACCAAATG
H04D03.3 Forward (for 8.3kb WT fragment)	CATCCGGGCCGCAGTATAAGAACAATTCAACCG
H04D03.3 Reverse (for 8.3kb WT fragment)	GCGCCTGCAGCGATTTGATAAAGTGCTTGAAAC